地学雑誌　Journal of Geography (Chigaku Zasshi)　130(1) 117–141 2021　doi:10.5026/jgeography.130.117

The 100s: Significant Exposures of the World (No. 12)

The Taupō Eruption Sequence of AD 232 ± 10 in Aotearoa New Zealand: A Retrospection

David J. LOWE* and Adrian PITTARI*

[Received 9 June, 2020; Accepted 13 August, 2020]

Abstract

The Taupō eruption, also known as eruption Y, occurred in late summer to early autumn (typically late March to early April) in AD 232 ± 10 yr at Taupō volcano, an 'inverse' caldera volcano underlying Lake Taupō in the central Taupō Volcanic Zone, North Island, Aotearoa New Zealand. The complex rhyolitic eruption, the most powerful eruption globally in the last 5000 years, lasted between several days and several weeks and generated five markedly contrasting pyroclastic fall deposits (units Y1 to Y5) followed by the extremely violent emplacement of a low-aspect-ratio ignimbrite (unit Y6). The fall deposits include three phreatomagmatic units, Y1, Y3, and Y4, the latter two being the products of archetypal phreatoplinian events; and two magmatic units, Y2 and Y5, the latter being the product of an exceptionally powerful plinian (previously described as 'ultraplinian') event with an extreme magma discharge rate around 10^8 to 10^{10} kg s^{-1}. The pyroclastic fall-generating eruptions were followed by the climactic emplacement of the entirely non-welded Taupō ignimbrite (Y6). It was generated by the catastrophic collapse of the 35 to 40-km-high plinian eruption column (Y5) that produced a very-fast-moving (600 to 900 km h^{-1}), hot (up to 500°C) pyroclastic flow (density current) that covered about 20,000 km^2 of central North Island over a near-circular area ~160 km in diameter, centred on Lake Taupō, in fewer than about ten to 15 minutes. This violent ground-hugging pyroclastic flow generated its own air lubrication, forming a near-frictionless basal region, and the resultant highly fluidised ignimbrite was spread as a near-continuous but thin sheet over the entire landscape, both infilling valleys and mantling ridges. Caldera collapse formed a new basin in the older Ōruanui caldera in Lake Taupo. The pressure-wave arising from the plinian-column collapse probably generated a global volcano-meteorological tsunami. Studied intensely by extraordinary volcanologists Colin Wilson and George Walker, and others, the exceptionally well-preserved and readily-accessible Taupō eruptives provide a one-in-a-hundred classic sequence that is arguably the most informative in the global world of volcanology with respect to explosive rhyolitic eruptions and their products. The total volume of the Taupō eruptives amounts to ~35 km^3 as magma, equivalent to ~105 km^3 of bulk (loose) pyroclastic material, of which the Taupō ignimbrite comprises ~30 km^3. The impacts and landscape response of the eruption were profound, spatially extensive, and enduring, and the young glassy soils (Vitrands in *Soil Taxonomy*, Pumice Soils in the *New Zealand Soil Classification*) developed in the silica-rich pumiceous deposits, although well suited to plantation forestry (especially exotic *Pinus radiata*), pose unique problems for agriculture and other land uses, including a high susceptibility to gully erosion and an inherent deficiency in cobalt and other trace elements, and require special management.

* School of Science, University of Waikato, Private Bag 3105, Hamilton 3240, Aotearoa New Zealand

Key words : Taupō eruption, Taupō supervolcano, eruption Y, non-welded ignimbrite, low-aspect ratio ignimbrite, inverse volcano, pyroclastic flow, density current, plinian, phreatoplinian, radiocarbon wiggle-matching, breakout flood, rhyolite, tephrochronology, tephra, Vitrands, Pumice Soils, volcanic hazard, Taupō Volcanic Zone, gullying, cobalt deficiency, plantation forestry

I. Introduction

Taupō caldera volcano comprises a complex of large caldera and fault structures in the central part of the Taupō Volcanic Zone (TVZ) (Figs. 1 and 2). The most frequently erupting and productive rhyolite volcano on Earth (Wilson *et al*., 2009), Taupō supervolcano is submerged by Lake Taupō, the largest fresh-water lake in Australasia. The volcano is an archetypal inverse volcano, which are concave with the 'flanks' sloping gently inwards towards the vent locations (Walker, 1981a, 1984). It overlies a very large silicic magmatic system (Barker *et al*., 2021). Volcanic events have been so voluminous and explosive, and the eruptives dispersed so widely, that the accumulation of material around the vents has not compensated for collapse associated with caldera formation (Wilson and Walker, 1985; Barker *et al*., 2021). Consequently, the bed of Lake Taupō in the vicinity of Horomatangi Reefs near the eastern shore (Fig. 2), at a depth of 185 m, is the lowest point in the landscape for over 40 km in any direction (Grange, 1937; Froggatt, 1979; Lowe and Green, 1992; Wilson, 1994).

The Taupō eruption, which took place in AD 232 ± 10 (see Section V below), was the latest of 27 eruptions to have taken place at Taupō volcano since the Ōruanui super-eruption occurred c. 25,400 calendar (cal.) years BP (Wilson, 1993, 2001, 2008; Houghton *et al*., 2010; Allan *et al*., 2012; Vandergoes *et al*., 2013; Dunbar *et al*., 2017). Also known as the Kawakawa event, the Ōruanui eruption was extremely voluminous with a total magma volume of ~530 km^3 (equivalent to ~1170 km^3 as bulk pyroclastic material) (Wilson, 2001). Caldera collapse associated with this huge eruption generated

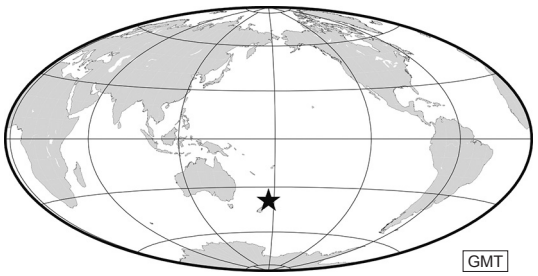

Fig. 1 Locality index of Taupō volcano, Aotearoa New Zealand.

the wide east-west ovoid basin that forms the northern part of Lake Taupō today (Wilson, 2001) (Fig. 2). The lake's southern basin is a syn-eruptive volcano-tectonic collapse structure relating to the Ōruanui eruption (Davy and Caldwell, 1998; Wilson, 2001; Allan *et al*., 2012; Barker *et al*., 2021).

II. Taupō eruption and its products

The ~AD 232 Taupō eruption, known as eruption Y in the post-Ōruanui stratigraphic sequence erected for Taupō volcano by Wilson (1993), was one of the most violent and complex rhyolite eruptions in the world in the past 5000 years (Wilson and Walker, 1985; Barker *et al*., 2016). The second or third largest eruption globally in the past 2000 years, the Taupō eruption is unique in the post-Ōruanui sequence in that it generated new caldera collapse, and its volume greatly exceeds (by about five times) those of any of the preceding (post-Ōruanui) eruptives (Barker *et al*., 2021). The Taupō eruption was centred on at least three vents on a northeast-southwest aligned fissure in the vicinity of the Horomatangi Reefs within eastern Lake Taupō (Fig. 2) (Smith and Houghton, 1995a; Houghton *et al*., 2003, 2010). The erup-

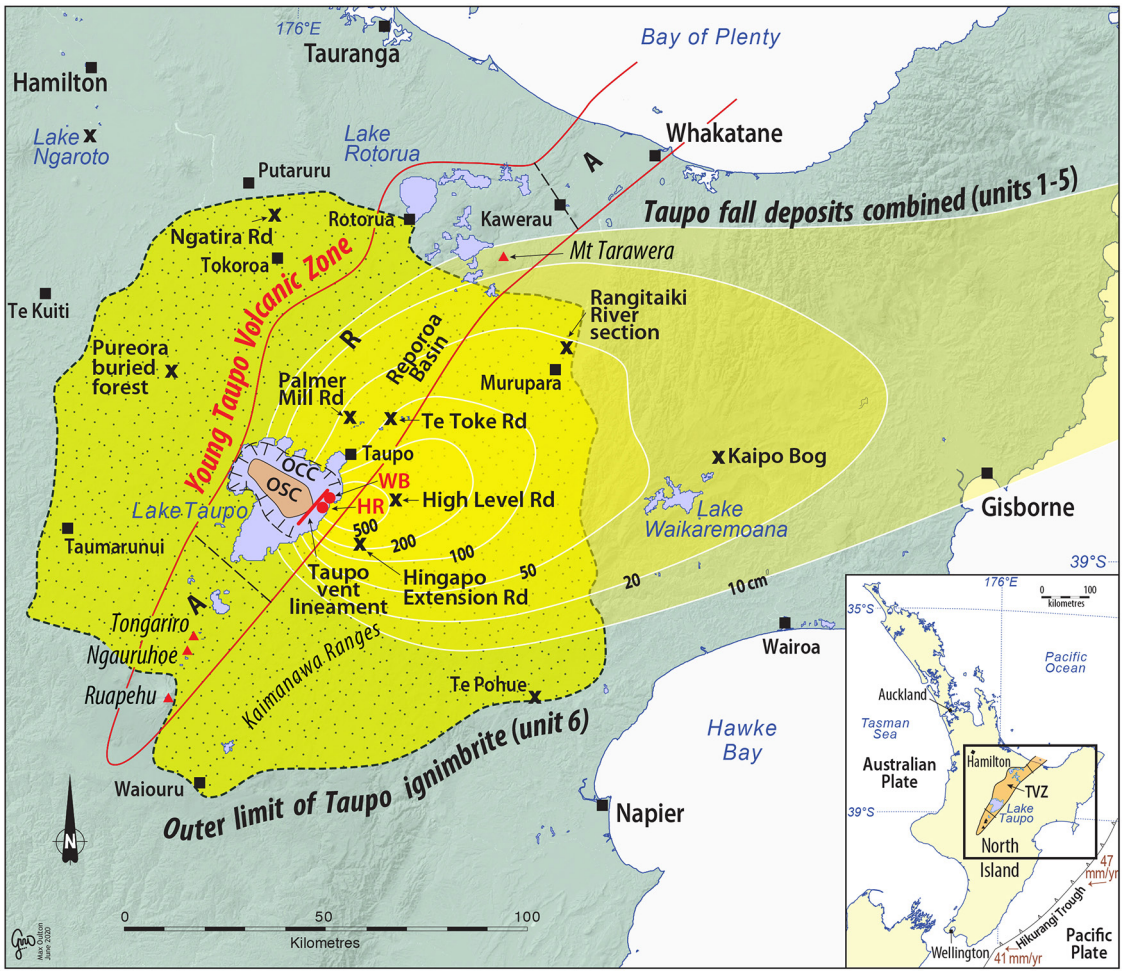

Fig. 2 Map of the central North Island showing the distribution of pyroclastic eruptives from the Taupō eruption (of AD 232 ± 10) comprising the tephra-fall deposits combined and the non-welded Taupō ignimbrite (after Wilson and Walker, 1985). Their source is the Taupō vent lineament now submerged in Lake Taupō near the subaqueous rhyolite domes of Horomatangi Reefs (HR) and Waitahanui Bank (WB) (Smith and Houghton, 1995a, 1995b; Houghton *et al*., 2010; von Lichtan *et al*., 2016). The lake occupies a caldera formed by the Ōruanui eruption c. 25,400 cal. yr BP: OSC, Ōruanui structural caldera; OCC, Ōruanui collapse collar (Wilson *et al*., 2006; Barker *et al*., 2016, 2019, 2021). Inset shows the plate tectonic setting of North Island (Leonard *et al*., 2010). The (Young) Taupō Volcanic Zone (TVZ), similar in size to the Yellowstone system but more productive (Houghton *et al*., 1995), is divided into a central rhyolitic part (R) flanked by zones dominated contrastingly by andesitic stratovolcanoes (A) (Wilson *et al*., 1984, 1995; Wilson and Rowland, 2016).

tion has been divided into seven contrasting phases, each of which generated diverse, but overwhelmingly pyroclastic, eruption products. The products have been given both stratigraphic names and equivalent unit designations, Y1 to Y7 (Fig. 3). Prior to 2003, the eruption was divided into units Y1 to Y7 followed by a separate event denoted as eruption Z, namely the subaqueous growth of lava domes (which generated large floating blocks) (Wilson, 1993). However, Houghton *et al*. (2003) revised the stratigraphic associations as follows: (i) erup-

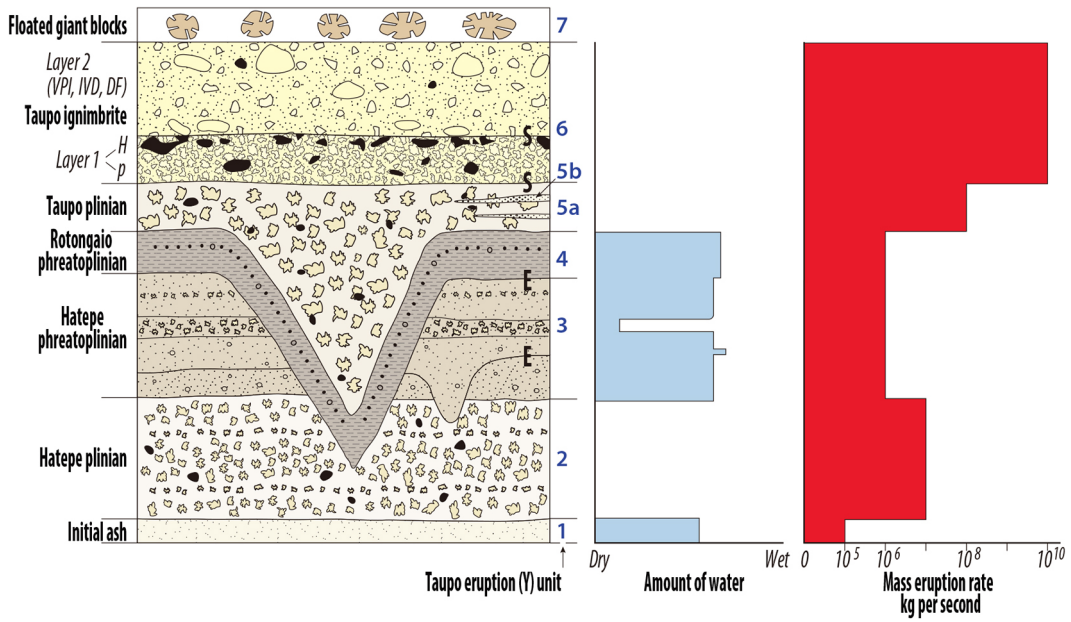

Fig. 3 Summary of the stratigraphy of deposits of the Taupō eruption (Unit Y) showing both stratigraphic names and volcanological unit designations (after Wilson and Walker, 1985; Houghton and Wilson, 1986; Houghton *et al*., 2003, 2010). Facies of Taupō ignimbrite are also shown: Layer 1, facies H and P; Layer 2, facies VPI, valley-ponded ignimbrite; IVD, ignimbrite veneer deposit; and DF, distant facies. Unit 7 comprises giant floated pumiceous blocks derived from subaqueous lava domes. Most symbols represent pumiceous clasts of varying grain size; solid symbols denote lithics (± crystals). Graphs at right indicate semiquantitative changes in the inferred degree of magma-water interaction and the magma discharge rate (which becomes extreme before and during emplacement of unit 6, Taupō ignimbrite). E and S denote, respectively, erosional horizons formed by running water (E) or shearing (S) beneath the fast-moving pyroclastic flow that deposited the non-welded Taupō ignimbrite (after Walker, 1981c; Houghton and Wilson, 1986; Wilson, 1994; Houghton *et al*., 2003, 2010).

tion Z was re-designated as the final effusive dome-growing stage, Y7, of the Taupō eruption sequence; (ii) the original units Y5 (Taupō plinian pumice) and Y6 (early ignimbrite flow units) were re-designated as units Y5a (Taupō plinian pumice) and Y5b (intra-plinian ignimbrite flow units), respectively; and (iii) the original unit Y7 was re-designated as Y6 (Taupō ignimbrite). The current stratigraphic names and units, used throughout this article, follow Houghton *et al*. (2003, 2010) and are summarised in Fig. 3. We mainly use the term pyroclastic ('fiery fragments') rather than tephric, its near synonym (Lowe, 2011), because of the volcanological focus of this paper.

We note that the Taupō eruption pre-dates human arrival in Aotearoa New Zealand by around 1000 years, the earliest Polynesian seafarers arriving around AD 1280, a few decades before the Kaharoa eruption of AD 1314 ± 12 (Hogg *et al*., 2003; Wilmshurst *et al*., 2008; Lowe, 2011; Lowe and Pittari, 2014). Consequently, the Taupō pyroclastic deposits provide an isochronous tephrochronological benchmark well before any human arrival and impacts (Lowe *et al*., 2000, 2002; Lowe and Newnham, 2004).

The eruption sequence consists of five explosive phases, two of them 'wet' or phreatomagmatic (i.e. involving magma-water interactions) and three 'dry' or magmatic (i.e. driven by expansion of internal volatiles), that deposited pyroclastic fall deposits (denoted as units Y1 to Y5), followed by the sixth and climactic plinian,

caldera-forming event that resulted in the subsequent emplacement of the non-welded Taupō ignimbrite (unit Y6) (Fig. 3). After some years or a decade or so, lava was extruded on to the bed of the reconfigured Lake Taupō, forming subaqueous domes comprising Horomatangi Reefs and Waitahanui Bank (Fig. 2). Large pumiceous blocks (forming unit Y7) broke away from the dome carapaces and floated to the lake surface before being driven ashore at multiple sites on the eastern side of the lake at levels up to 10 m higher than those of today (Wilson and Walker, 1985; Smith, 1991; Wilson, 1993; Manville *et al*., 1999; von Lichtan *et al*., 2016).

The eruption pyroclastic fallout deposits greater than 10 cm in thickness cover ~30,000 km^2 of land in the eastern North Island and the ignimbrite covers a near-circular area of ~20,000 km^2 (Fig. 2). The fall deposits from the eruption comprise one of the most varied sequences yet described from a single eruption episode, and the emplacement of the Taupō ignimbrite is regarded as the most violently emplaced pyroclastic flow deposit yet recorded (Wilson and Houghton, 2004). Barker *et al*. (2021) noted that the Taupo eruption pyroclastic deposits are regarded as type examples globally because of their widely varying eruptive styles.

The total volume of the Taupō eruptives is at least 35 km^3 as magma, equivalent to ~105 km^3 of bulk pyroclastic material, a figure that includes co-ignimbrite ashfall and material beneath the waters of Lake Taupō (Wilson and Walker, 1985; Wilson, 1993).

1) Significant exposure: Taupō eruptives Y2 to Y6 at High Level Road section, east Taupō

Five of the Taupō eruptive units are exposed at a spectacular section on High Level Road east of Lake Taupō, ~20 km from the vent (Fig. 2). The section is shown in Fig. 4.

2) Taupō eruption sequence phase by phase

The Taupō eruption in its entirety lasted between several days and several weeks (Wilson and Walker, 1985). The dispersals of eruptives generated by each phase are shown on six maps (Fig. 5) on which the location of the section at High Level Road (Fig. 4) is denoted by a grey star.

2-1) Phase 1

The eruption began with relatively minor phreatomagmatic activity, with cold lake water mixing with hot magma to generate the fine-grained Initial ash (unit Y1) over a period of a few hours, and from an eruption column ~10 km high (Wilson and Walker, 1985), so that the distribution is relatively localised (Fig. 5). The volume of phase 1 eruptives is estimated to be ~0.05 km^3 as loose material (Wilson, 1993).

2-2) Phase 2

The Hatepe plinian deposits (unit Y2) represent a change to largely magmatic activity and a step-up in eruption intensity, expressed as mass eruption rate (Fig. 3), so that an eruption column ~30 km high was formed and the airborne pyroclasts were blown over considerable distances (Fig. 5) (Wilson and Walker, 1985). Early dilute density currents and minor late-stage pyroclastic flows (density currents) were also generated (Talbot *et al*., 1994; Houghton *et al*., 2010). The fall deposits are faintly bedded although appearing to be uniform and well sorted and represent an average, moderately-sized plinian eruption (Walker, 1981b) with an estimated volume of ~2.5 km^3 as loose material (Wilson, 1993).

2-3) Phase 3

The Hatepe phreatoplinian ash (unit Y3) is a predominantly fine-grained, crudely bedded deposit that is putty-like when wet, and it readily becomes sensitive or thixotropic (Walker, 1981c). Rich in fine-grained, highly-vesicular pumice clasts, the eruption marks a period when vent-widening allowed abundant external water, including lake water, to gain access to the rising and erupting gas-charged magma. In addition, steam would have been generated in substantial amounts, condensing to produce rain, which flushed ash out of the eruption column/plume so that it fell as wet sticky mud, being found draped over branches of shrubs or trees preserved in the deposits (Walker, 1981c; Smith and Houghton, 1995b; Wilson and Hough-

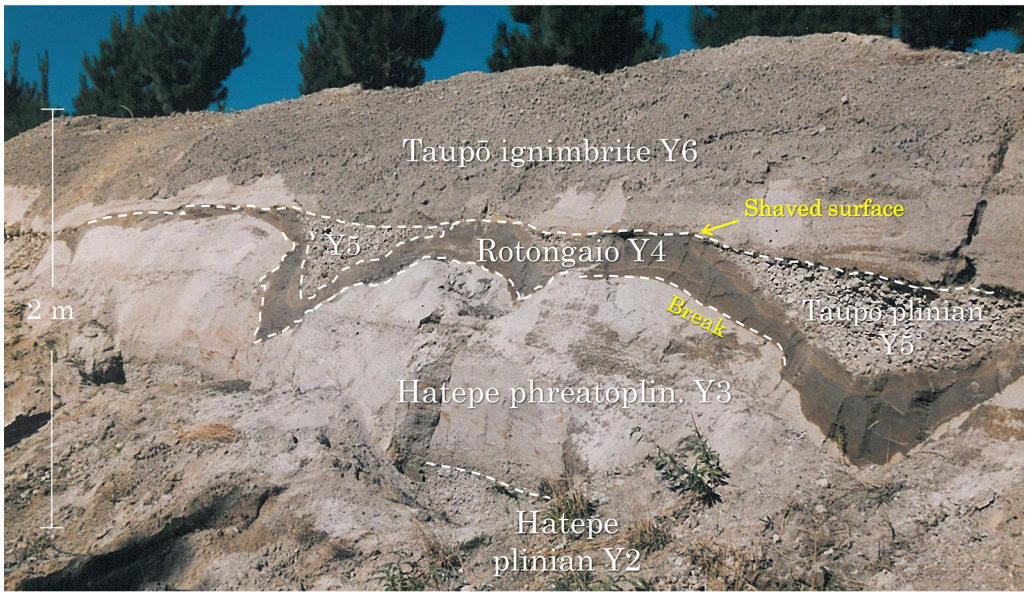

Fig. 4 Section on High Level Road (Fig. 2) showing contrasting pyroclastic deposits of the Taupō eruption including both 'wet' and 'dry' fallout deposits (units Y2 to Y5) and unconsolidated Taupō ignimbrite (unit Y6). The Hatepe (Y2) and Taupō (Y5) plinian materials are notably coarser than those of the two fine-grained phreatoplinian events (Y3 and Y4), with the coarsest deposits of Taupō plinian attesting to the extreme power of the Y5 phase of the eruption. The 'break' refers to a period of possibly hours to fewer than about three weeks in duration (Walker, 1981c; Wilson and Walker, 1985; Wilson, 1993) during which pre-existing Hatepe phreatoplinian deposits (Y3) were eroded by erupted lake water, probably together with runoff from rainstorms, into shallow gullies or rills so that the subsequent fine-grained mantling deposits of the Rotongaio phreatoplinian deposits (Y4) form a striking V-shaped pattern. Smith and Houghton (1995a) argued, however, that there was essentially no break between the emplacement of Y3 and Y4. An earlier erosional event took place during the Hatepe phreatoplinian phase (Y3), although the shallow gullies generated by it (cut into Y2) are not as conspicuous (Walker, 1981c; Fig. 3). At the top of the section, the emplacement of the Taupō ignimbrite (Y6) by the unrestrained pyroclastic flow has shaved of most of the Y5 deposits except where they were protected in the erosional gullies (Houghton and Wilson, 1986). Site location: 38°47′56″S, 176°15′21″E. Photo: D.J. Lowe.

ton, 2004). Phase 3 was interrupted at least once by a brief return to 'dry' plinian activity, represented at the High Level Road section by a ~5 cm-thick pumice lapilli bed within unit Y3 (Fig. 3). The phreatomagmatic eruption, which endured for a few to tens of hours (Wilson and Walker, 1985), has been described as a typical or even archetypal phreatoplinian event (Smith and Houghton, 1995a; Kósik *et al*., 2019). Its products were blown eastwards (Fig. 5). Their volume is estimated to be ~1.9 km^3 as loose material (Wilson, 1993).

During, and immediately after, the phase 3 eruption, two breaks involving deposit erosion may have occurred (Fig. 3), the durations of which are uncertain. Estimates for the more prominent break at the end of phase 3 range from hours to fewer than about three weeks (Walker, 1981c; Wilson and Walker, 1985; Wilson, 1993), although Smith and Houghton (1995a) contrarily suggested that there was no significant time break between phase 3 and the ensuing phase 4. During the break at the end of phase 3, or during a period when phases 3 and 4 were erupting simultaneously from two different vents (see Fig. 5), intense rainfall resulted in the formation by erosion of shallow gullies or rills, about 1 m in depth on average, in tephra deposits east of Lake Taupō (Walker, 1981c). The rainfall was derived from either

voluminous ejected water or condensate from steam from Lake Taupō itself, or from a common meteoric storm, or both. The gullies deepen closer to Lake Taupō, where they may be 2 m or more deep (Walker, 1981c). Gullies that were probably formed to the south are inferred to have been removed by severe erosion during very intense rainfall, that water deriving ultimately from lake water near the vent that was jetted into the eruption plume (Smith and Houghton, 1995a).

2-4) Phase 4

The renewal of the eruption resulted in the deposition of the Rotongaio phreatoplinian ash (unit Y4) as a consequence of abundant lake water encountering a shallow subaqueous dome of dense, degassed magma that was exposed by the opening of a new vent to generate a dark-grey, very-fine-grained obsidian-rich ash that, like Y3, landed wet (Houghton *et al*., 2003; Wilson and Houghton, 2004). It infilled the eroded gullies to form a very distinctive V-shaped layer in the sequence (Figs. 3 and 4). The Rotongaio phreatoplinian ash is markedly fine grained with little material coarser than 1 mm, even in the most proximal exposures (Kósik *et al*., 2019), and the unit contains numerous intra-formational rills, some on a scale of 3 to 10 cm and others 40 cm wide and 30 cm deep, produced by syn-eruptive erosion (Smith and Houghton, 1995a). An erupted volume, as loose material, for the unit is estimated at ~1.1 km^3 (Wilson, 1993).

2-5) Phase 5

The fifth event in the sequence, Taupō plinian (Y5), saw an abrupt switch to a 'dry' and extremely powerful, magmatically-driven eruption, generating a towering column about 35 to 40 km high (Houghton *et al*., 2014) that deposited vesicular pumice over a very wide area, denoted unit Y5a (Fig. 5). The eruption intensity reached near-extreme values with magma discharge between 8×10^4 to 2.4×10^5 m^3 s^{-1} (approximately 10^8 kg s^{-1}: Houghton *et al*., 2003, 2010) (Fig. 3). At least 11 modest- or small-volume, intra-plinian pyroclastic flow deposits (density currents) were erupted co-evally, denoted as unit Y5b (Fig. 5), both proximal (weakly-emplaced, metre-thick) and distal (energetically-emplaced, decimetre-thick) deposits associated with partial collapse of the plinian column or relatively gentle overflow from the vent (Wilson and Walker, 1985; Wilson, 1993; Houghton *et al*., 2010). The majority of the pumice was blown eastwards across the country and well beyond Hawke's Bay into the Pacific Ocean. As well as this extreme dispersal, the plinian fall deposits (Fig. 6), which have a maximum observed thickness of only 2.1 m, show a very slow rate of thinning with distance from vent, the slowest yet recorded for a 'dry' fall deposit (Wilson, 1993).

These features—the wide dispersal, high magma eruption rate, and extreme eruption style—led Walker (1980) to describe the Taupō eruption (phase 5a) as 'ultraplinian', a new and unique end-member class at the time. He suggested that such a powerful eruption, which he estimated as lasting between six and 17 hours, would have generated an eruption column 50–55 km high, at the theoretical limit. However, Wilson and Walker (1985) estimated an eruption column 30 to 40 km in height, and Houghton *et al*. (2014) suggested that a column 35 to 40 km high—still at the top end of the plinian range (Trolese *et al*., 2109)—was likely. Phase 5a of the eruption generated ~7.7 km^3 of loose material (Wilson, 1993) (a larger volume of 23 km^3 was estimated, using a mass-balance method, by Walker, 1980), and phase 5b has an estimated volume, as loose material, of ~1.5 km^3 (Wilson, 1993).

2-6) Phase 6

The sixth and climactic phase of the Taupō eruption was the extremely violent emplacement of the Taupō ignimbrite, the product of a hot, excessively fast-moving, ground-hugging pyroclastic flow (within the spectrum of pyroclastic density current types) formed by the catastrophic collapse of the plinian column of phase 5a. As well as vent widening and ground subsidence, generating a new caldera manifested as a sub-rectangular basin within the older Ōruanui collapse structure (Davy and Caldwell,

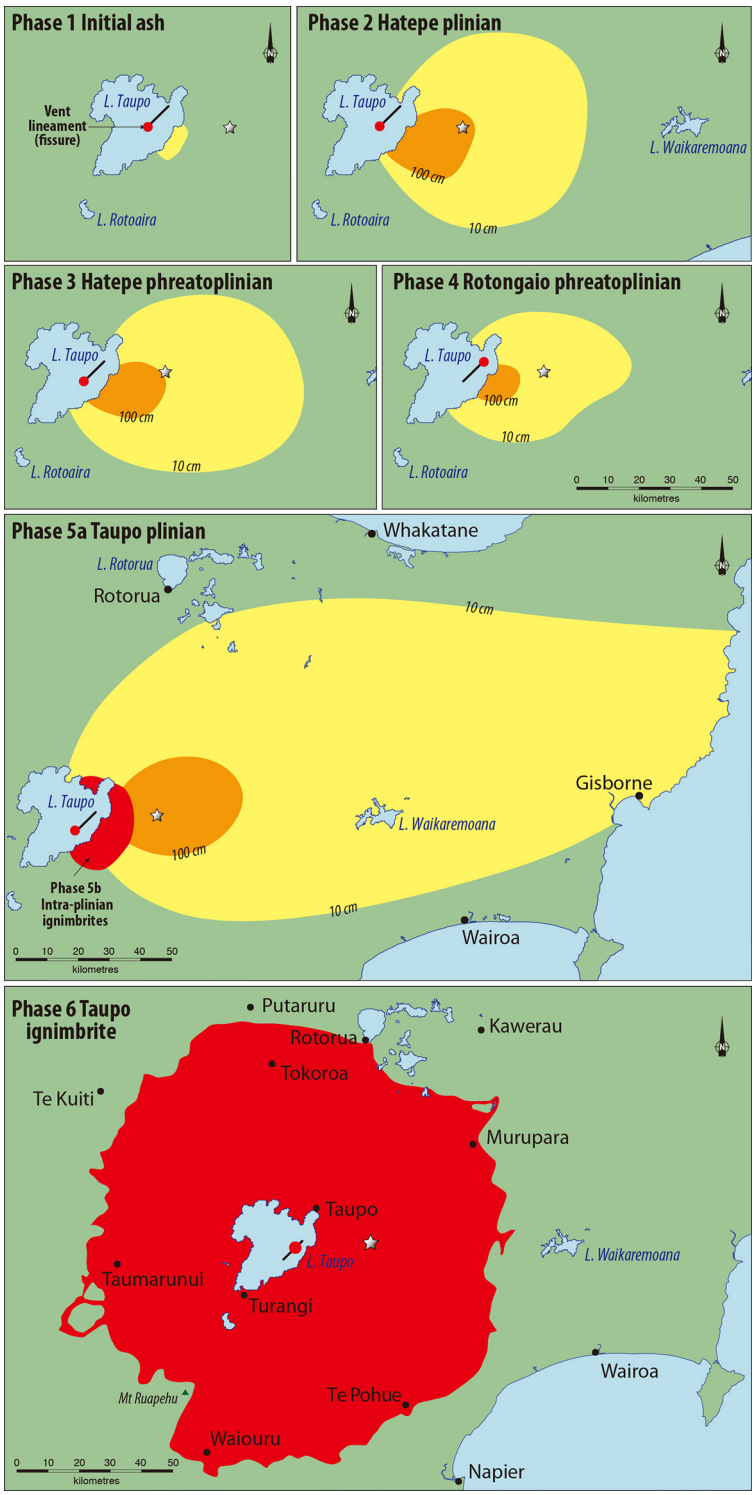
Phase 1 Initial ash
Vent lineament (fissure)
L. Taupo
L. Rotoaira
Phase 2 Hatepe plinian
L. Taupo
100 cm
10 cm
L. Rotoaira
L. Waikaremoana
Phase 3 Hatepe phreatoplinian
L. Taupo
100 cm
10 cm
L. Rotoaira
Phase 4 Rotongaio phreatoplinian
L. Taupo
100 cm
10 cm
L. Rotoaira
0 10 20 30 40 50
kilometres
Phase 5a Taupo plinian
Whakatane
L. Rotorua
Rotorua
10 cm
Gisborne
L. Taupo
100 cm
L. Waikaremoana
Phase 5b Intra-plinian ignimbrites
10 cm
Wairoa
0 10 20 30 40 50
kilometres
Phase 6 Taupo ignimbrite
Putaruru
Rotorua
Kawerau
Tokoroa
Te Kuiti
Murupara
Taupo
L. Taupo
L. Waikaremoana
Taumarunui
Turangi
Wairoa
Mt Ruapehu
Te Pohue
Waiouru
Napier
0 10 20 30 40 50
kilometres

Fig. 5

1998; Manville *et al*., 1999), the column collapse was caused by a drastic change in eruption conditions. The inferred extremely high discharge rate of 10^8 to 7×10^{10} kg s^{-1} (Fig. 3) was much greater than that capable of forming a stable plinian column (Wilson and Walker, 1981, 1985; Houghton *et al*., 2003, 2010; Trolese *et al*., 2019). From modelling, Dade and Huppert (1996) suggested that the rate of magma discharge was 5×10^7 m^3 s^{-1}. They calculated the temperature of ejecta in the eruption column was 700°C, the vertical velocity was 300 m s^{-1}, and that the vent had a radius of almost 1 km (see also Dade and Huppert, 1997; Wilson, 1997).

The pyroclastic flow was so energetic, in part because of the extreme explosivity of the eruption, that it travelled radially outwards from Lake Taupō at speeds of around 200 to 300 m s^{-1} (approximately 600 to 900 km h^{-1}), or greater near vent, for about 80 ± 10 km in all directions (Wilson and Walker, 1982; Wilson, 1985, 1993; Dade and Huppert, 1996). The velocity remained high (> 100 m s^{-1}) towards the outer limits of the flow. From ~40 km outwards the flow was a single wave of material and it stopped only when the material ran out (Walker *et al*., 1981b; Wilson and Walker, 1985). The pyroclastic flow, with a volume of ~30 km^3 (as loose material), covered an area of 20,000 km^2 in around 400 seconds (7 minutes) (Wilson and Walker, 1985). Dade and Huppert (1996) suggested from an isothermal hydraulic model that the entire emplacement took no more than 15 minutes. The high speed and fluidity gave the flow sufficient momentum to allow it to easily surmount mountains > 1500 m high, including Tongariro (1978 m above sea level, asl) and high peaks on the Kaimanawa Range (up to 1727 m asl), with only Ruapehu (2797 m asl) high enough to block it (Figs. 2 and 5). Large-scale laboratory simulations and modelling have recently shown that pyroclastic flows generate their own air lubrication, forming a near-frictionless basal region displacing particles upwards, thereby allowing huge masses (thousands to millions of tonnes) of material to be transported over uneven and upsloping terrains such as that in central North Island (Lube *et al*., 2019).

During its passage the pyroclastic flow consisted of a head, strongly fluidized by ingested air and the near-frictionless basal zone, which generated layer 1 deposits, and a body plus tail, which generated layer 2 (Fig. 6; Wilson and Walker, 1985). Layer 1 comprises two facies, a pumice-rich facies P, termed jetted deposits, which are overlain by a dense, lithic- and crystal-rich facies H, termed the ground layer (Walker *et al*., 1981a, b; Wilson, 1985). Layer 1 deposits underlie layer 2, which consists of mainly pumiceous materials dominated by coarse clasts (lapilli, blocks) and abundant fine material (ash) (Fig. 6). As noted further below, layer 2 is manifested as two pumiceous facies: valley-ponded ignimbrites and ignimbrite veneer deposits (Walker *et al*., 1981b; Wilson, 1985). In many places, layer 1 is depleted in fine material, described as fines-depleted ignimbrite, its turbulent emplacement and ingestion of timber (see below) likely leading to the depletion of finer vitric constituents so that it is clast-supported for all clasts exceeding ~2 mm in size (Walker *et al*., 1980b; Wilson and Walker,

Fig. 5 Maps showing the distribution of the pyroclastic fall and flow deposits that were emplaced during the six explosive phases of the Taupō eruption (Fig. 3). The maps are based mainly on Wilson and Houghton (2004). Maps 1–4 have the same scale. The positions of three recognised vents (red dots) lying on the 9-km-long NE–SW fissure or lineament in Lake Taupō are based on Wilson (1993), Smith and Houghton (1995a), and Houghton *et al*. (2003). The grey star marks the location of the section shown in Fig. 4. In terms of hazards, the yellow zones received 10 to 100 cm of fall deposits, which would destroy roofs on most houses, especially if wet. The orange zones received > 100 cm of fall deposits, which would be uninhabitable. The red zones were covered by ignimbrite, and the pyroclastic flows that emplaced them would have destroyed all life and structures in their path. For a more sophisticated analysis of potential ash-dispersal-related hazards, see Barker *et al*. (2019).

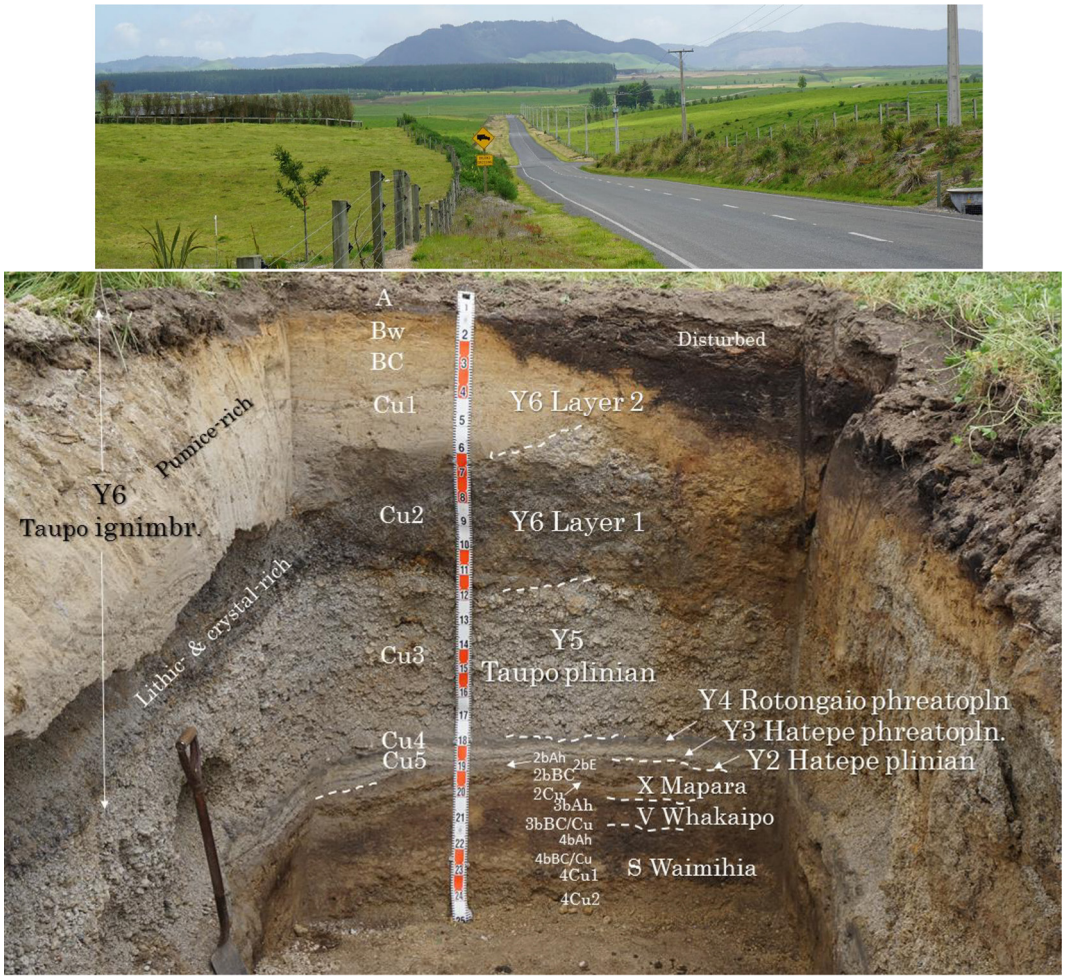

Fig. 6 Upper photo. Typical subdued (gently rolling to flat or undulating) Taupō-eruptive-mantled landscape of the central TVZ, viewed looking west along Te Toke Road, with steep rhyolite domes in far distance. The pit was excavated on near-flat ground to the far right on farmland (Endeavour Farm), ~30 km north of the vent (Fig. 2). The two main land uses for these glassy pumiceous soils are evident: agriculture and plantation forestry. Lower photo. The base of the section comprises three pre-Taupō tephras and associated paleosols (Wilson, 1993): unit S, Waimihia (3382 ± 50 cal. yr BP); unit V, Whakaipo (2800 ± 60 cal. yr BP); and unit X, Mapara (2059 ± 118 cal. yr BP) (ages from Lowe *et al*., 2013). These beds are overlain by three thin (≤ 5 cm) early Taupō-eruption units Y2–Y4. In turn, Y4 is overlain by ~0.7 m of Taupō plinian deposits (unit Y5), above which is ~1.2 m of Taupō ignimbrite (unit Y6) with the contrasting lithologies of layers 1 and 2 clearly expressed. Layer 1 (mainly facies H, a fines-depleted ground layer) is so loose that parts of the pit wall at left have fallen down. Layer 2 represents the IVD facies. Pedological horizonation is also shown (based on Clayden and Hewitt, 1994) and the young soil's classification is given in Section IV. Section-tape units are decimetres. Site location: 38°34′29″S, 176°14′28″E (nearby road cuttings show similar features). Photos: D.J. Lowe.

1985). The properties of layer 2 show a wide spectrum of lateral variants (Wilson and Walker, 1985): proximal deposits are coarse grained, with large lithic clasts, whereas distal deposits are often very fine grained and almost wholly pumiceous and, moreover, contain very low-density pumice. The differing lateral variations are mainly a result of the upward movement

of fine, light, dominantly pumiceous material within the flow in response to strong fluidization, and the unfurling of the flow because of its extreme violence so that the upper parts of the flow travelled the farthest (Walker and Wilson, 1983; Wilson, 1985; Wilson and Walker, 1985).

The emplacement of the Taupō ignimbrite resulted in sudden and dramatic changes to large parts of the central North Island landscape. The pre-ignimbritic fall beds (units 1–5) had blanketed the antecedent land as a landscape-modifying (i.e. mantling) event, making it smoother. In contrast, the emplacement of the Taupō ignimbrite was primarily a landscape-forming event in that the flows infilled valleys (including deposits, left behind from the flow body, partially draining back into valleys) and blocked them off, destroying surface hydrologic networks (Wilson, 1985; Manville *et al*., 1999). Taupō ignimbrite is thus thicker in valleys, forming the valley-ponded ignimbrite deposits (VPIs) between ~1 and 70 m deep, typically $\geq$ 5 m, and with flat to gently undulating surfaces (Fig. 7A) (Walker *et al*., 1981b; Wilson, 1985; Manville *et al*., 2009). The thicknesses of the VPIs are independent of the distance from vent (Wilson and Walker, 1982, 1985). As the flow crossed topographic highs, climbing slopes as steep as 30°, it emplaced thin ignimbrite-veneer deposits (IVDs), 0.25 to 8 m deep, typically 0.5 to 2 m in thickness (Fig. 7A) (Walker *et al*., 1981b; Wilson and Walker, 1985). The IVDs systematically decrease in thickness with distance from vent, with distal deposits (> 40 km from vent) effectively comprising a continuous IVD (Walker *et al*., 1981a, b; Wilson and Walker, 1981; Wilson, 1985). Walker *et al*. (1981b) described the IVD as a deposit from a pyroclastic flow, recording its passage as a 'trail-marker' while the flow has continued on, whereas the VPI is the trailing part of the body of the flow itself that has come to rest.

The distal deposits (termed the distant facies, DF) represent the lateral equivalent of layer 1 (P) and layer 2 on distant interfluves (Fig. 7C), and are interpreted to be flow-head and flow-body material that was mixed together and spread over the landscape as the flow ran out of material while still retaining a high velocity (Wilson and Walker, 1982; Wilson, 1985).

The ignimbrite covered a near-circular area and reached about the same distance after crossing several substantial mountain ridges as it did after travelling in other sectors over nearly level ground (Wilson, 1985). Rather than piling up around the vent (like the proximal early flow units of phase 5b) to generate a clearly defined ignimbrite surface, the Taupō ignimbrite to a large extent drapes the pre-existing landscape and in places superficially resembles a fall deposit (Fig. 7C; Wilson and Walker, 1985). The IVDs on high points in the landscape mimic the effect of fall beds in generally smoothing (rounding) the landscape contours (Healy, 1967).

Various other volcanological features relating to the ignimbritic deposit, which are everywhere non-welded, include the deposition of jetted deposits that represent layer 1 (P) facies (jets of material thrown forward supersonically from the advancing wave-like front of the flow head as a result of the violent expansion of ingested air), and in places the flow tore up or overturned parts of the underlying soil and incorporated them into the ignimbrite as rip-up clasts as well as scalping the antecedent Taupō plinian deposits of phase 5a (Fig. 4) (Wilson, 1985; Wilson and Walker, 1985). Many of the large pumice clasts are notably rounded because of transport in a pyroclastic flow. In the fall deposits, the size of the pumice clasts generally decreases with distance from the eruption source (those of the Taupō plinian phase being exceptionally slow to diminish, as noted earlier) while the proportion of fine-ash particles typically increases with distance from source. Pumice clasts in the pyroclastic flow deposits, however, show a complex relationship of size with distance from source that depends on the source of the deposit: clasts in the IVDs (on ridge tops) decrease in size away from source but those in the VPIs (in antecedent valleys) remain uniform or increase slightly in size away from source to about 40 km from vent

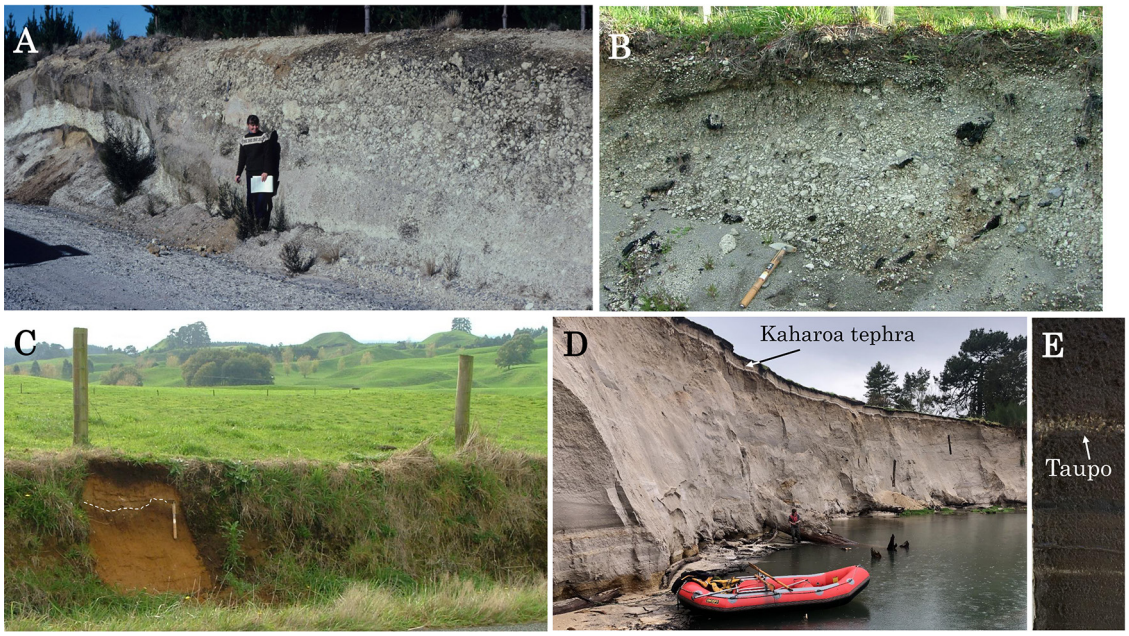

Fig. 7 A. Exposure of Taupō ignimbrite on Hingapo Extension Road, 19 km southeast from vent (Fig. 2), showing two facies: at right is a valley-ponded ignimbrite (VPI) (> 3 m thick) which morphs laterally to the far left into an ignimbrite-veneer deposit (IVD) overlying a pre-ignimbrite paleosol (marked by the yellow-brown soil under the white pumice) on a low hill (see Wilson, 1985, plate 6: Fig. 34a). The VPI contains a coarse-grained pumice concentration zone overlain by fine deposits ~0.5 m thick (darkened zones) at the land surface (Houghton and Wilson, 1986). Site location: 41°25′38″S, 172°08′47″E. Photo: D.J. Lowe. B. Taupō ignimbrite (Y6) exposed on Palmer Mill Road, ~25 km north of vent, showing abundant charcoal and carbonised logs. Cutting tool is 30 cm long. Site location: 38°35′15″S, 176°04′40″E. Photo: D.J. Lowe. C. Pumice-dominated, distant-facies deposit of non-welded Taupō ignimbrite (above the dashed line) in a gently rolling to hilly landscape on Ngatira Road near Lichfield, ~75 km north of vent and barely 5 km from the flow's outermost margin (Fig. 2). The steeper hills and semi-continuous plateaux in far background comprise much older welded ignimbrite sheets ~1 Ma in age that have been partly dissected by erosion (Lowe and Pittari, 2019). The Taupō ignimbrite is ~0.5 m thick and is underlain by a buried paleosol on multiple thin pre-Taupō eruptives. Scattered fine pumice lapilli at the base of the ignimbrite may represent Taupō plinian material (Y5a). Cutting tool is 30 cm long. Site location: 38°06′28″S, 175°49′29″E. Photo: D.J. Lowe. D. Thick (~9 m) pumice-rich fluvial deposits mainly comprising debris flow and hyperconcentrated flow materials emplaced within a few years of the Taupō eruption (Manville *et al*., 1999, 2005, 2009), and exposed alongside the Rangitāiki River near Murupara (Fig. 2) in the Galatea depression. The fluvial deposits overlie a remnant buried forest (note in situ stumps and logs at river level) and are capped by bright-white rhyolitic Kaharoa tephra-fall materials erupted from Mt Tarawera in AD 1314 ± 10 (Hogg *et al*., 2003). Site location: 38°25′40″S, 176°42′7″E. Photo: E. Smeith. E. Photo showing ~5 to 10-mm-thick layer of fine lapilli/coarse ash of the Taupō eruption, possibly representing deposition of co-ignimbrite fallout material, preserved in dark organic rich lake sediments in Lake Ngaroto, near Hamilton (Fig. 2), and ~110 km northwest and 'upwind' from the vent (Lowe, 1988). Site location: 38°57′12″S, 175°17′20″E. Photo: D.J. Lowe.

until decreasing beyond 60 km from vent (Wilson, 1985).

The extreme violence and fluidity of the relatively dilute Taupō pyroclastic flow caused the ignimbrite to be spread as an effectively continuous but thin sheet over the entire landscape with an average thickness of about 1.5 m (Walker *et al*., 1980b), only being broken where locally cut by later erosion (Walker *et al*., 1981b). Such a thin but widespread sheet is referred to as a low-aspect-ratio ignimbrite, the aspect ratio being the vertical dimension divid-

ed by the horizontal dimension—in this case ~1: 100,000 (Walker *et al*., 1980a; Walker and Wilson, 1983). Despite its thinness and thus innocuous appearance, the Taupō ignimbrite reflects the most extreme of dangers in the spectrum of volcanic hazards (Walker, 1980) as a function of its very high mobility and heat (Breard *et al*., 2019). Because of its violence and energy release ($\geq 150 \pm 50$ megaton TNT explosive yield, cf. Hiroshima bomb 0.015 Mt), and by analogy with the AD 1883 Krakatau eruption episode, it is probable that the Taupō ignimbrite-emplacement phase generated a volcano-meteorological tsunami (essentially the collapsing eruption column displaced a large volume of air laterally, forming pressure waves) that may have reached coastal areas worldwide (Lowe and de Lange, 2000).

The Taupō pyroclastic flow engulfed and carbonised an entire forest, ingesting about 1 km^3 of timber in total (Hudspith *et al*., 2010), and charred logs and charcoal are ubiquitous in the ignimbrite (Fig. 7B). The carbonized logs have been measured at up to 1 m in diameter close to vents, and 5 m in length (Froggatt *et al*., 1981; Hudspith *et al*., 2010). The trees were broken off by the pyroclastic flow or preceding blast, and then incorporated into the hot flow. Their pattern of orientation radially around the eruption source vent provided a means of mapping its position in the vicinity of the Horomatangi Reefs (Fig. 2; Froggatt, 1979; Froggatt *et al*., 1981). Further evidence was provided by Walker (1980). Before then, the explicit vent position for the eruption had been uncertain, with locations both in and beyond the lake having been suggested (Froggatt, 1981a). As well, until the charcoal-bearing units were identified as a pyroclastic flow deposit (rather than fall), it had been a puzzle as to how the deposit had remained so hot throughout its 160-km-wide distribution (Grange, 1937). It seems Baumgart and Healy (1956) were the first to infer that the uppermost part of the deposit ('Upper Taupo Pumice') (Layer 2 today) originated from a primary pyroclastic flow that was 'laid down by glowing avalanches that hugged the lower ground, and accompanied periodic explosive eruptions of great magnitude' (p.122). Terms such as 'ash flows', 'huge *nuées ardentes*', and 'glowing avalanches' were also used in the 1950s–60s to describe the origin of the uppermost deposit (e.g. Baumgart, 1954; Baumgart and Healy, 1956; Healy, 1965, 1967). Gibbs (1968) described the final Taupō eruptives as originating from 'extremely hot clouds of material [that] were blasted across the land, burning vegetation and sweeping logs, soil, and ash into depressions' (p.10). Estimates from charring experiments by Hudspith *et al*. (2010) and from thermal remanent magnetic work by McClelland *et al*. (2004) indicate the ignimbrite's temperature was 400 to 500°C at sites beyond 40 km from vent, and 150 to 300°C at sites within 30 to 40 km of the vent. Beyond the zone of ignimbrite emplacement, forests located up to 170 km east of the vents were damaged to a varying degree by pyroclastic fall deposits, and fires were evident during the eruption, continuing afterwards for several decades (Wilmshurst and McGlone, 1996; Horrocks and Ogden, 1998). Changes in forest composition before and after the eruption were also recorded by Clarkson *et al*. (1995).

Originally the term 'ignimbrite' (meaning 'fiery storm-clouds'), introduced by Marshall in the 1930s (1932, 1935), was associated by implication with hard (welded) rocks (Cole *et al*., 1972; Lowe and Pittari, 2019). It took many decades for unconsolidated or non-welded pyroclastic flow deposits to be recognised also as 'legitimate' ignimbrites, with Sparks *et al*. (1973) providing the first definition to that end. Walker (1980), Walker *et al*. (1980a, b, 1981b), and Froggatt (1981a) were the first to name the Taupō pyroclastic flow deposit specifically as the 'Taupō ignimbrite', with Froggatt (1981a) summarising evidence for its flow origin in a 12-point list.

The approximately equivalent Layer 2 and Layer 1 deposits were previously called 'Upper Taupo Pumice' and 'Rhyolite Block Beds', respectively (see Froggatt, 1981a, and Wilson and Walker, 1985, for summaries of historical no-

menclature).

2-7) Phase 7

At some stage after the cessation of the climactic eruption of Taupō ignimbrite, possibly after an interval of several years to a few decades, rhyolite lava domes were erupted (extruded) onto the floor of the re-formed Lake Taupō (Wilson and Walker, 1985) at a rather modest magma discharge rate of ~10^3 kg s^{-1} (Houghton *et al*., 2010). These domes are manifested as the submerged Horomatangi Reefs and Waitahanui Bank within the modern lake (Fig. 2), which together comprise a volume of 0.28 km^3 (volume as lava: Wilson, 1993). The domes are draped in glassy pumiceous rhyolite debris (Wilson, 1993; von Lichtan *et al*., 2016). Scattered large pumiceous, glassy rhyolite blocks, of metre to decametre dimension, the largest around 17 m in length, occur on a wave-cut terrace along the eastern shoreline ~5 m above present-day lake level. They are inferred to have spalled from carapaces on one or more of the submerged rhyolite domes and then floated ashore, being driven eastward by the prevailing westerlies some time after the explosive phases (Wilson and Walker, 1985; Wilson and Houghton, 2004; Barker *et al*., 2021). Palaeomagnetic measurements by von Lichtan *et al*. (2016) show that the giant blocks were hot, above the Curie point, when they were gently emplaced, and the well-preserved chilled contact and jointing features on them support this evidence (Barker *et al*., 2021). The giant blocks became embedded in accumulating transgressive shore-face sediments and continued cooling (von Lichtan *et al*., 2016). The chemical composition of lava from the Horomatangi Reefs matches those of the Taupō eruptives and the floated giant blocks, confirming their coeval origins (Barker *et al*., 2015, 2021).

The floated blocks thus represent the youngest material erupted (unit Y7) during the Taupō eruption sequence (Fig. 3). Their grounding at a lake level higher than that of today implies that the lake must have refilled after the close of explosive activity, which would have taken possibly around ten to 30 years (estimates range from 'several years to a decade' to possibly 30 or 40 years: Wilson and Walker, 1985; Smith, 1991; Manville *et al*., 1999; Houghton *et al*., 2010; Barker *et al*., 2021). Because of blockage of its outlet, the new lake attained a mean high-stand ~390 m asl, about 34 m above its present level (357 m asl), marked by a semi-continuous wave-cut bench and shoreline deposits (Manville, 2002; Manville *et al*., 2007). As the exit channel (Waikato River) was re-established (see Section III below), the lake fell cataclysmically, forming a wave-cut bench at 368–371 m asl (i.e. ~5 m above present level) (Grange, 1937; Wilson and Walker, 1985; Manville *et al*., 1999, 2007), the site on which the giant floated pumices became stranded. Wilson and Walker (1985, p.213) described one such block as coming to rest on post-Taupō-eruption lake sediments, slightly deforming them prior to being buried by younger sediments before the lake fell to its present-day position.

3) Co-ignimbrite ash deposits

Co-ignimbrite ash deposits (equivalent to layer 3 of Sparks *et al*., 1973) associated with the emplacement of Taupō ignimbrite have not been commonly observed nor described, being restricted to a few widely scattered outcrops beyond the outer limit of the ignimbrite (Wilson and Walker, 1985). Nevertheless, Manville (2002) and Manville *et al*. (2009) reported that, although volumetrically insignificant, the co-ignimbrite layer, representing fallout from the elutriated-ash plume suspended above the pyroclastic flow, as well as distal remnants of the plinian eruption plume, and inferred to have been deposited within a few hours of the emplacement of Taupō ignimbrite, is an important stratigraphic marker between syn- and early post-Taupō eruptive reworking.

Thin distal deposits in lakes and peats, such as shown in Fig. 7E, less than ~5 cm or so in thickness and distributed well off the strongly eastward-directed axis of the ≥ 10-cm-thick Taupō fall beds (Fig. 2), may represent co-ignimbritic ash fallout, as inferred by Lowe (1988) for around six Late Quaternary tephra deposits in the Waikato region that are seeming-

ly thicker than the exponential would predict. Pullar *et al*. (1977, p. 698) show a near-circular 5-cm-thick isopach of 'Taupo Pumice' (centred approximately on Rotorua) that contrasts with the west-east orientated fall-out isopach pattern of Wilson and Walker (1985). Barker *et al*. (2019) have modelled ash dispersal from radially expanding umbrella clouds, and concluded that with increasing eruption size (using five scenarios, the Taupō event falling between scenarios 3 and 4 with respect to magma volume), the formation of an umbrella cloud may propel significant amounts of ash upwind and crosswind as the cloud/plume becomes less sensitive to the weather conditions as a result of the increasing role of density-driven dispersal in the plume. Such a scenario may help explain the pattern of fallout shown by Pullar *et al*. (1977) and others for distal Taupō tephra deposits.

III. Post-Taupō-eruption reworking and impacts on landscape

The immediate aftermath of the eruption would have seen erosion, secondary deposition, and reworking by water, wind, and gravity on a massive scale over large areas of central North Island and beyond. The rivers draining the 160-km-wide zone around Taupō, choked with fall deposits and Taupō ignimbrite, acted as major pathways for reworking and flooding after the eruption (Wilson and Walker, 1985). Using a combined stratigraphical, sedimentological, and geomorphological approach, Manville (2002) and Manville *et al*. (2009) described the landscape response to the Taupō eruption as a distinct four-stage sequence (stages 0 to III), but with overlap between each (i.e. post-eruption stages I to III were diachronous). Although the general remobilisation pattern is similar for all impacted river systems, the relative timing and extent of each response stage differ for each of the Waikato, Rangitaiki, Mohaka, Ngaruroro, and Whanganui catchments, reflecting differences in physiography and hydrology and the volume and type of pyroclastic material deposited in each (Segschneider *et al*., 2002; Manville *et al*., 2009).

Stage 0 is associated with the eruption itself and emplacement of the successive fall beds and the Taupō ignimbrite, the expulsion of water from Lake Taupō, and the modification and formation of new landscapes, including landscape inversion and transformations of drainage, as described earlier. Some remobilisation of primary deposits would have occurred before deposition of the co-ignimbrite ash layer (Manville, 2002).

Stage I is a period (spanning hours to a few years) of early remobilisation of the barren duvet of fine-grained, pumice-rich pyroclastic deposits over an area $> 20{,}000$ km^2 (Fig. 2), especially where the vegetation had been entirely destroyed or buried. Frequent rainstorms would have caused intense erosion and deposition of the easily entrained loose and low-density pumice materials (Selby and Hosking, 1973), involving mainly mass flows, and rilling and gullying on slopes, with flash flooding generating downstream aggradation by debris and hyperconcentrated flow deposits (Manville, 2002).

Stage II was a period of fluvial re-establishment lasting several months to years, as upland rill networks stabilised and sediment yields decreased as rills or gullies deepened sufficiently to encounter soil-covered paleo-land surfaces with less-easily-eroded materials. Temporary lakes were formed, including the extensive supra-ignimbrite paleo-Lake Reporoa (in the Reporoa basin: Fig. 2), which formed in about three years and had a maximum area of ~190 km^2 and a volume of ~2.5 km^3 (Manville, 2001). The lake would have emptied quickly after overtopping the barrier at its lowest point, near Orakei Korako, generating a peak flood discharge of about 17,000 m^3 s^{-1} which contrasts with the Waikato River flow rate through the area today of ~130 m^3 s^{-1} (Manville, 2001). Gullies deepened into box canyons in the ignimbrite valley fill deposits (VPIs) via headward erosion (Healy, 1967), and water flow in shallow ephemeral streams, carrying hyperconcentrated flows (e.g. Fig. 7D), became permanent rather than episodic as sediment

loads declined so that the rivers became deeper and braided, eventually (over years to decades) returning to pre-eruption gradients and bedloads (Segschneider *et al*., 2002; Manville, 2002; Manville *et al*., 2009).

Stage III is the period beginning with the Taupō breakout-flood (initiated approximately 20 years after the eruption) through to the present day. As described above (section on phase 7 of the eruption), blockage of the outlet gorge of the Waikato River by a natural dam 30 to 40 m high, comprising non-welded pumiceous pyroclastic deposits (remnants of these are still evident today on valley walls and in tributaries), resulted in the post-eruption overfilling of the Taupō lake basin over a period of some decades to a level ~34 m above that of the present day (Manville *et al*., 1999, 2007; Manville, 2002). Catastrophic failure of the pyroclastic dam by overtopping because of rising lake waters led to the re-establishment of the Waikato River, choked with Taupō ignimbrite, and the release of ~20 km^3 of impounded water in a single phase, the peak discharge rate being estimated at 15,000–30,000 $m^3\ s^{-1}$, with a total flood duration of 1 to 4 weeks (Manville *et al*., 1999). Such a discharge rate is equivalent to that of the modern Mississippi River in flood (Manville *et al*., 1999). The flood was highly erosive near its source in proximal areas, forming a deep trench or spillway through the VPI deposits before emerging into basins such as Reporoa where it deposited coarse-grained alluvial fans (Manville, 2002). In medial and distal areas, the flood deposits aggraded the valley floors, eventually forming terraces underlain with deposits termed Taupō Pumice Alluvium that can be traced ~230 km downstream of Lake Taupō (Selby and Lowe, 1992). Parts of Hamilton and Whanganui cities, for example, are built on these deposits alongside the present Waikato and Whanganui rivers, respectively. Manville (2002) makes the point that remobilization of pyroclastic material can persist for decades after an eruption to affect areas well beyond the initial impacted zone, and that the range and duration of the sedimentary response is therefore one of the most significant of volcanic hazards.

IV. Formation of glassy soils on Taupō eruptives and their special character

The soils formed in the unconsolidated rhyolitic Taupō eruptives, emplaced barely 1800 years ago, are youthful and only weakly weathered with a low clay content ($\leq$ ~5%) in uppermost horizons, and most clay is allophane (Lowe and Palmer, 2005; McDaniel *et al*., 2012). Their main physical properties tend to be dominated by the glassy, vesicular, coarse textures and low-density ($<$ 1 g cm^{-3}) pumice constituents. However, the soils show some differences spatially according to variations relating to the diverse Taupō eruption fall and flow deposits and their distance from source, and the soils on the VPIs tend to be dense and tightly-packed, with subsoils potentially brittle and compact, resisting penetration by plant roots (Gibbs, 1968; Rijkse and Vucetich, 1980). In some places with suitable drainage situations, subsoils can be weakly cemented with secondary silica (P.L. Singleton *pers. comm.*, 2020; Hewitt *et al*., 2021).

Equivalent pumice-rich soils are developed on the Taupō Pumice Alluvium flanking the Waikato, Whanganui, and other rivers (Lowe, 2010).

Most soils on the Taupō eruptives are classified as Pumice Soils at order level in the *New Zealand Soil Classification* (NZSC; Hewitt, 2010), and in *Soil Taxonomy* (ST; Soil Survey Staff, 1999) they are usually classed as a 'vitric' suborder within the Andisols, namely the Vitrands (Lowe and Palmer, 2005; McDaniel *et al*., 2012). They are designated as a separate order (i.e. at the highest level) in NZSC because of their wide extent in central North Island (covering ~15.5% of North Island's total land area), their special character (physically, mineralogically, and chemically), and particular land-management requirements. The soil profile shown in Fig. 6 is an excellent example, being classified as an Immature Orthic Pumice Soil in NZSC (Hewitt, 2010), and as a Typic Udi-

vitrand in ST (Lowe *et al*., 2014; Soil Survey Staff, 2014). At higher elevations under podocarp-dominated forest and with increasing leaching, strongly acid Podzol Soils (NZSC) or Spodosols (ST) form on the Taupō ignimbrite and associated deposits (Grange and Taylor, 1932; Lowe and Palmer, 2005; Palmer *et al*., 2005).

The Taupō rhyolitic pumice, notably enriched in silica (70 to 78 wt% SiO_2), has low quantities of major nutrient elements and soils are likely to be deficient in trace elements including cobalt, copper, molybdenum, boron, iodine, and selenium. For productive agriculture, such as dairying, it is necessary to add fertiliser and trace elements, particularly cobalt because its deficiency causes a serious and usually fatal 'wasting disease' of sheep and cattle relating to a lack of vitamin B_{12} (Scott and Molloy, 2012; Hewitt *et al*., 2021). The exotic Monterey pine (*Pinus radiata*) has been successfully grown on Pumice Soils in large numbers mainly since the 1920s, and the pines thrive, particularly when their roots are able to delve into nutrients and moisture stored in subsurface paleosols. Because of the pumice's low bulk density and weak coherence, Pumice Soils are readily eroded by water, with gullying a specific risk, and need to be protected by vegetation cover (Selby, 1972).

V. Dating the Taupō eruption

1) Year

The Taupō ignimbrite contains copious charcoal and carbonised logs (Fig. 7B) and hence it was a prime target when the capacity to undertake radiocarbon (^{14}C) dating in New Zealand was developed in the early 1950s. The first ^{14}C date to be published in New Zealand was on charcoal from the Taupō ignimbrite, NZ-1: 1820 ± 150 ^{14}C yr BP (68% probability range) (Fergusson and Rafter, 1953; Grant-Taylor and Rafter, 1963). Since then, more than ~70 samples from Taupō eruptives have been dated from charcoal and wood, and from a wide range of other carbonaceous materials including peat, lake sediment, seeds, and leaves (e.g. Healy, 1964; Hogg *et al*., 1987; Froggatt and Lowe, 1990). However, changes in dating methodology over the past 60 years, differing pretreatment regimes, modified age-calculation procedures, and potential errors associated with sample types, such as in-built age and stratigraphic superpositioning, together with wiggles and plateaux in the calibration curves, have meant that the date of the eruption has been elusively imprecise (Hogg *et al*., 2019). For example, based on a set of seven ^{14}C ages obtained on optimal (short-lived) leaves and seeds preserved at the Pureora buried forest (Fig. 2; see below), Lowe and de Lange (2000) were able to determine only a broad calendar date for the eruption spanning nearly 200 years: AD 130–320 (95% probability range).

Meanwhile, other estimates for the age of the eruption had been suggested including an ice-core-derived age of ~AD 181 (e.g. Zielinski *et al*., 1994), and a purported historical link dated at ~AD 186 associated with atmospheric perturbations (extended sunsets) recorded in ancient Rome and China supposedly caused by the Taupō eruption (Wilson *et al*., 1980). In the ice-core studies, however, the sulphate spikes picked out as being derived from the Taupō eruption were not verified by geochemical fingerprinting because no glass shards were detected in the acid layers, and the curious atmospheric phenomena were disputed by Froggatt (1981b) and Stothers and Rampino (1983) (Hogg *et al*., 2012).

A solution to deriving a much more precise date arose from a serendipitous event stemming from the eruption itself. During the collapse of the plinian eruption column to generate the pyroclastic flow, the (tsunami-generating) pressure wave of the air preceding the flow, or the passage of the flow front itself, felled the forest (before the trees were engulfed in ignimbrite) at Pureora, ~50 km northwest of the vent (Fig. 2). The flattened forest at Pureora was then perfectly preserved by peat development because of the ensuing alteration in drainage (Clarkson *et al*., 1988; Palmer *et al*., 1988; Hogg *et al*., 2012; Watts *et al*., 2019) (Fig. 8A). To circumvent the uncertainty arising from the

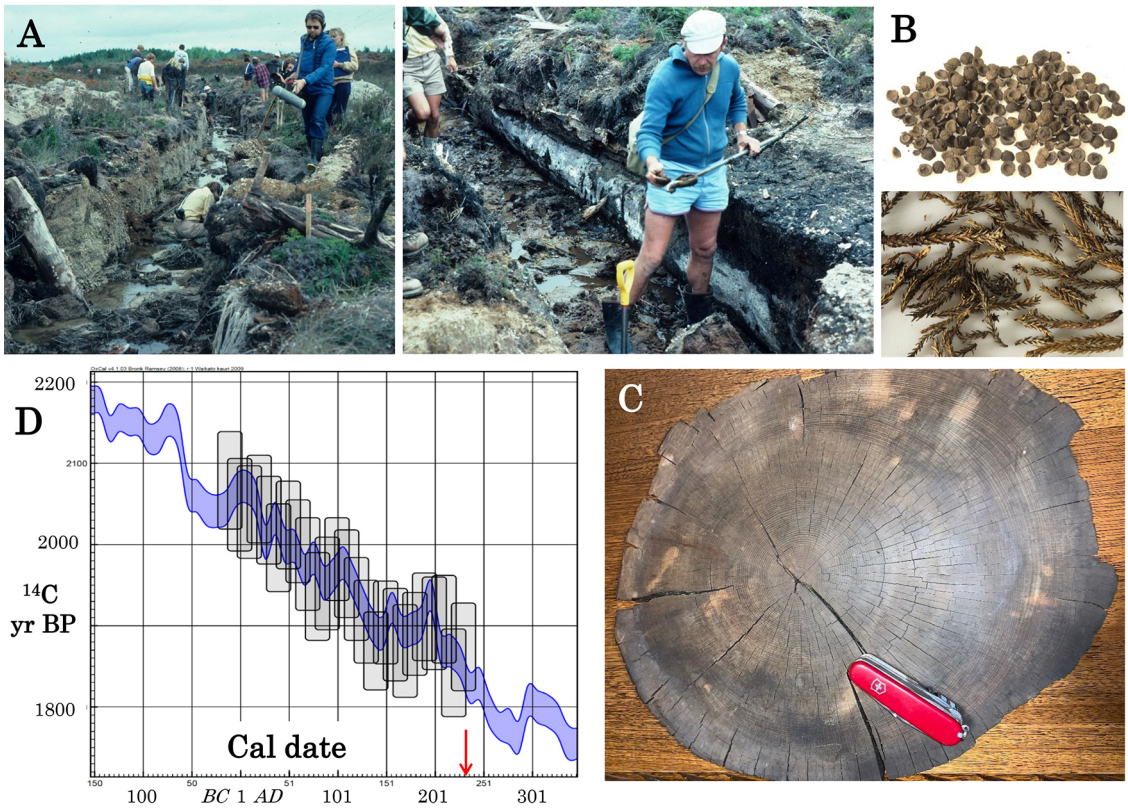

Fig. 8 A. Two views of the soon-to-be famous buried forest, under Taupō ignimbrite and peat, at Pureora on 14 February, 1984 (Fig. 2). Ditches expose trees flattened in the blast. Site location: approximately 38°30′S, 175°35′E. Photos: D.J. Lowe (leftmost photo after King *et al*., 2015). B. Preserved tree seeds (top image) of mātai (*Prumnopitys ferruginea*) and miro (*P. taxifolia*) and leaves (bottom image) of rimu (*Dacrydium cupressinum*), collected and identified by B.R. Clarkson in 1984 and used for dating by Lowe and de Lange (2000). Photos: D.J. Lowe (after King *et al*., 2015). C. Slab of tanekaha (*Phyllocladus trichomanoides*) used to determine the date of the Taupō eruption using ^{14}C wiggle-match dating (Hogg *et al*., 2012, 2019). Penknife is ~10 cm long. Photo: J. Palmer. D. Twenty-five contiguous decadal dates (grey boxes) from the tanakeha log fitted against the kauri-derived calibration curve (blue) for New Zealand. The date at AD 232 (red arrow) is derived from the calibration curve informed by the fit of all the decadal dates against it (after Hogg *et al*., 2012).

inter-hemispheric offset in the ^{14}C calibration curves, Hogg *et al*. (2012) developed a high-precision New Zealand-derived ^{14}C calibration curve using dendrochronology and samples of kauri (*Agathis australis*), a long-lived conifer native to northern New Zealand. A large log from Pureora of celery pine, tanekaha (*Phyllocladus trichomanoides*) (Fig. 8C), was then sampled dendrochronologically to generate 25 high-precision ^{14}C dates from a sequence of 25 decadal samples, pre-treated to form α-cellulose. The suite of contiguous dates was then statistically wiggle-matched against the kauri calibration curve (Fig. 8D) to derive a new, more precise calendar date of AD 232 ± 10 years (95% probability range).

The wiggle-match ^{14}C date of ~AD 232 was supported by an independent estimate made using Bayesian age-depth modelling at Kaipo bog (Fig. 2), where stratigraphically ordered, independent age points (37 local ^{14}C ages and 16 tephrochronological ages) were used to

derive a date for the Taupō layer in the Kaipo peat of AD 231 ± 12 (OxCal software) and AD 251 ± 51 (weighted-mean date AD 240) (Bacon software) (Lowe *et al*., 2013), statistically identical to the Pureora wiggle-match estimate. A similar date of AD 231/232 for the Taupō eruption event was inferred by Sigl *et al*. (2013) using sulphate signals (with a sulphate flux [SO_4^{2-}] range from 13 to 15 kg km^{-2}) in annually-dated ice cores from both Greenland (core NEEM S1) and Antarctica (core WDC06A), i.e. the two sulphate spikes are recorded at exactly the same time in both hemispheres, referred to as bipolar occurrence. The annual minimum sulphur values are above the natural background in the ice for up to seven consecutive years, indicating a moderate but long-lasting flux of volcanogenic sulphur, which Sigl *et al*. (2013) attributed to Taupō's high plinian eruption column (phase Y5a) penetrating the tropopause and hence injecting aerosols into the stratosphere to affect global dispersal (Wilson and Walker, 1985). Winstrup *et al*. (2019), working on another Antarctic ice core (RICE), reported a date for an (assumed) Taupō-eruption-derived sulphate spike of AD 236 ± 33. However, glass shards from the Taupō eruption have not yet been reported in any ice cores in Greenland nor Antarctica, and so the attribution of the ice-core sulphate signals at AD 231/232 to the Taupō eruption is unable as yet to be confirmed definitively (Sigl *et al*., 2013).

Although the work of Hogg *et al*. (2012) was recently challenged by Holdaway *et al*. (2018), further evaluations and revised calculations by Hogg *et al*. (2019) have confirmed the date of AD 232 ± 10 years.

2) Season

The Taupō eruption took place in late summer to early autumn (typically late March to early-middle April) on the basis of fruit and seeds preserved at Pureora (Clarkson *et al*., 1988) (e.g. Fig. 8B) and the lack of an outer latewood ring on preserved logs (Palmer *et al*., 1988). Preserved insect assemblages suggested the ignimbrite was deposited in the late afternoon (Clarkson *et al*., 1988).

Acknowledgements

We thank Eric Smeith for providing the photograph in Fig. 7D, Jonathan Palmer for the photograph in Fig. 8C, Colin Wilson for his assistance in unravelling the stratigraphy of deposits shown in Fig. 6, Alan Bullick for providing access to Endeavour Farm and for facilitating the excavation of the pit shown in Fig. 6, and Alan Hogg for providing Fig. 8D. Peter Singleton and Malcolm McLeod provided helpful information on soils formed on Taupō-derived VPIs. Max Oulton is thanked for preparing Figs. 2, 3, and 5, and Maria McGuire and others for accessing some key articles in less-than-readily-available journals/proceedings during the COVID-19 crisis lockdown of 2020. We thank Hiroshi Machida for his suggestion, and editor-in-chief Yukio Isozaki and former editor-in-chief Yohta Kumaki for their invitations to contribute this article to the special topic, "The 100s". A reviewer and the editor (Kenichiro Tani) are acknowledged and thanked for their very helpful comments. Kenichiro Tani also undertook the translations. The paper is an output of the Commission on Tephrochronology (COT) of the International Association of Volcanology and Chemistry of the Earth's Interior (IAVCEI).

References

Allan, A.S.R., Wilson, C.J.N., Millet, M.-A. and Wysoczanski, R.J. (2012): The invisible hand: Tectonic triggering and modulation of a rhyolitic supereruption. *Geology*, **40**, 563–566.

Barker, S.J., Wilson, C.J.N., Allan, A.S.R. and Schipper, C.I. (2015): Fine-scale temporal recovery, reconstruction and evolution of a post-supereruption magmatic system: Taupo (New Zealand). *Contributions to Mineralogy and Petrology*, **170**, 5.

Barker, S.J., Wilson, C.J.N., Morgans, D.J. and Rowlands, J.V. (2016): Rapid priming, accumulation, and recharge of magma driving recent eruptions at a hyperactive caldera volcano. *Geology*, **44**, 323–326.

Barker, S.J., Van Eaton, A.R., Mastin, L.G., Wilson, C.J.N., Thompson, M.A., Wilson, T.M., Davis, C. and Renwick, J.A. (2019): Modelling ash dispersal from future eruptions of Taupo supervolcano. *Geochemistry, Geophysics, Geosystems*, **20**, doi:10.1029/2018GC008152.

Barker, S.J., Wilson, C.J.N., Illsley-Kemp, F., Leonard, G.S., Mestel, E.R.H., Mauriohooho, K. and Charlier, B.L.A. (2021): Taupō: An overview of New Zealand's supervolcano. *New Zealand Journal of Geology and Geophysics*, doi:10.1080/00288306.2020.1792515.

Baumgart, I.L. (1954): Some ash showers of the central North Island. *New Zealand Journal of Science*

and Technology, **B35**, 456–467.
Baumgart, I.L. and Healy, J. (1956): Recent volcanicity at Taupo, New Zealand. *Proceedings of the 8th Pacific Science Congress* (held in The Philippines, November 1953), **2**, 113–125.
Breard, E.C.P., Jones, J.R., Fullard, L., Lube, G., Davies, C. and Dufek, J. (2019): The permeability of volcanic mixtures—Implications for pyroclastic currents. *Journal of Geophysical Research: Solid Earth*, **124**, doi:10.1029/2018JB016544.
Clarkson, B.R., Patel, R.N. and Clarkson, B.D. (1988): Composition and structure of forest overwhelmed at Pureora, central North Island, New Zealand, during the Taupo eruption (c. A.D. 130). *Journal of the Royal Society of New Zealand*, **18**, 417–436.
Clarkson, B.R., McGlone, M.S., Lowe, D.J. and Clarkson, B.D. (1995): Macrofossil and pollen representing forests of the pre-Taupo volcanic eruption (c. 1850 yr BP) era at Pureora and Bennydale, central North Island, New Zealand. *Journal of the Royal Society of New Zealand*, **25**, 263–281.
Clayden, B. and Hewitt, A.E. (1994): Horizon notation for New Zealand soils. *Division of Land and Soil Sciences Scientific Report*, **1**, 1–30.
Cole, J.W., Kohn, B.P., Pullar, W.A., Milne, J.D.G., Vucetich, C.G. and Healy, J. (1972): Pyroclastic nomenclature in New Zealand. *New Zealand Journal of Geology and Geophysics*, **15**, 686–692.
Dade, W.B. and Huppert, H.E. (1996): Emplacement of the Taupo ignimbrite by a dilute turbulent flow. *Nature*, **381**, 509–512.
Dade, W.B. and Huppert, H.E. (1997): Emplacement of Taupo ignimbrite. *Nature*, **385**, 307–308.
Davy, B.W. and Caldwell, T.G. (1998): Gravity, magnetic and seismic surveys of the caldera complex, Lake Taupo, North Island, New Zealand. *Journal of Volcanology and Geothermal Research*, **81**, 69–89.
Dunbar, N.W., Iverson, N.A., Van Eaton, A.R., Sigl, M., Alloway, B.V., Kurbatov, A.V., Mastin, L.G., McConnell, J.R. and Wilson, C.J.N. (2017): New Zealand supereruption provides time marker for the Last Glacial Maximum in Antarctica. *Scientific Reports*, **7**, 12238.
Fergusson, G.J. and Rafter, T.A. (1953): New Zealand ^{14}C age measurements I. *New Zealand Journal of Science and Technology*, **B35**, 127–128.
Froggatt, P.C. (1979): Lake Taupo—Probable source of Taupo Pumice Formation. *New Zealand Journal of Geology and Geophysics*, **22**, 763–764.
Froggatt, P.C. (1981a): Stratigraphy and nature of Taupo Pumice Formation. *New Zealand Journal of Geology and Geophysics*, **24**, 231–248.
Froggatt, P.C. (1981b): Did Taupo's eruption enhance European sunsets?. *Nature*, **293**, 491.
Froggatt, P.C. and Lowe, D.J. (1990): A review of late Quaternary silicic and some other tephra formations from New Zealand: Their stratigraphy, nomenclature, distribution, volume, and age. *New Zealand Journal of Geology and Geophysics*, **33**, 89–109.
Froggatt, P.C., Wilson, C.J.N. and Walker, G.P.L. (1981): Orientation of logs in the Taupo Ignimbrite as an indicator of flow direction and vent position. *Geology*, **9**, 109–111.
Gibbs, H.S. (1968): Volcanic-ash soils in New Zealand. *New Zealand Department of Scientific and Industrial Research Information Series*, **65**, 30p.
Grange, L.I. (1937): The geology of the Rotorua-Taupo subdivision, Rotorua and Kaimanawa divisions. *New Zealand Department of Scientific and Industrial Research Geological Survey Bulletin*, **37**, 138p.
Grange, L.I. and Taylor, N.H. (1932): The occurrence of bush sickness on the volcanic soils of the North Island. A. The distribution and field characteristics of bush-sick soils. *New Zealand Department of Scientific and Industrial Research Bulletin*, **32**, 21–35.
Grant-Taylor, T.L. and Rafter, T.A. (1963): New Zealand natural radiocarbon measurements I–V. *Radiocarbon*, **5**, 118–162.
Healy, J. (1964): Dating of the younger volcanic eruptions of the Taupo region. Part 1. *New Zealand Geological Survey Bulletin*, **73**, 7–39.
Healy, J. (1965): Trends in New Zealand volcanology. *New Zealand Journal of Geology and Geophysics*, **8**, 1127–1138.
Healy, J. (1967): Recent erosion in Taupo Pumice, central North Island, New Zealand. *New Zealand Journal of Geology and Geophysics*, **10**, 839–854.
Hewitt, A.E. (2010): *New Zealand Soil Classification, 3rd edition. Landcare Research Science Series*, **1**, 136p.
Hewitt, A.E., Balks, M.R. and Lowe, D.J. (2021): Pumice Soils. in *The Soils of Aotearoa New Zealand*. Springer, Cham, 179–198.
Hogg, A.G., Lowe, D.J. and Hendy, C.H. (1987): University of Waikato radiocarbon dates I. *Radiocarbon*, **29**, 263–301.
Hogg, A.G., Higham, T.F.G., Lowe, D.J., Palmer, J., Reimer, P. and Newnham, R.M. (2003): A wiggle-match date for Polynesian settlement of New Zealand. *Antiquity*, **77**, 116–125.
Hogg, A.G., Lowe, D.J., Palmer, J.G., Boswijk, G. and Bronk Ramsey, C.J. (2012): Revised calendar date for the Taupo eruption derived by ^{14}C wiggle-matching using a New Zealand kauri ^{14}C calibration data set. *Holocene*, **22**, 439–449.
Hogg, A.G., Wilson, C.J.N., Lowe, D.J., Turney, C.S.M., White, P., Lorrey, A.M., Manning, S.W., Palmer, J.G., Bury, S., Brown, J., Southon, J. and Petchey, F. (2019): Wiggle-match radiocarbon dating of the Taupo eruption. *Nature Communications*, **10**, 4669.
Holdaway, R.N., Duffy, B. and Kennedy, B. (2018): Evidence for magmatic carbon bias in ^{14}C dating of the Taupo and other major eruptions. *Nature Communications*, **9**, 4110.

Horrocks, M. and Ogden, J. (1998): The effects of the Taupo Tephra eruption c. 1718 BP on the vegetation of Mt Hauhungatahi, central North Island, New Zealand. *Journal of Biogeography*, **25**, 649–660.

Houghton, B.F. and Wilson, C.J.N. (1986): Explosive rhyolitic volcanism: the case studies of Mayor Island and Taupo volcanoes. *New Zealand Geological Survey Record*, **12**, 33–100.

Houghton, B.F., Wilson, C.J.N., McWilliams, M.O., Lanphere, M.A., Weaver, S.D., Briggs, R.M. and Pringle, M.S. (1995): Chronology and dynamics of a large silicic magmatic system: Central Taupo Volcanic Zone, New Zealand. *Geology*, **23**, 13–16.

Houghton, B.F., Hobden, B.J., Cashman, K.V., Wilson, C.J.N. and Smith, R.T. (2003): Large-scale interaction of lake water and rhyolitic magma during the 1.8 ka Taupo eruption, New Zealand. in *Explosive Subaqueous Volcanism* edited by White, J.D.L., Smellie, J.L. and Clague, D.A., *Geophysical Monograph*, **140**, 97–109.

Houghton, B.F., Carey, R.J., Cashman, K.V., Wilson, C.J.N., Hobden, B.J. and Hammer, J.E. (2010): Diverse patterns of ascent, degassing, and eruption of rhyolite magma during the 1.8 ka Taupo eruption, New Zealand: Evidence from clast vesicularity. *Journal of Volcanology and Geothermal Research*, **195**, 31–47.

Houghton, B.F., Carey, R.J. and Rosenberg, M.D. (2014): The Taupo eruption: "Ill wind" blows the ultraplinian type event down to Plinian. *Geology*, **42**, 459–461.

Hudspith, V.A., Scott, A.C., Wilson, C.J.N. and Collinson, M.E. (2010): Charring of woods by volcanic processes: an example from the Taupo ignimbrite, New Zealand. *Palaeogeography Palaeoclimatology Palaeoecology*, **291**, 40–51.

King, C.M., Hay, J.R., Smale, M.C., Leathwick, J.R. and Beveridge, A.E. (2015): Forest and native wildlife. in *The Drama of Conservation—The History of Pureora Forest, New Zealand* edited by King, C.M., Gaukrodger, D.J. and Ritchie, N.A., Springer, Berlin, and New Zealand Department of Conservation, Wellington, 19–42.

Kósik, S., Voloschina, M., Zemeny, A., Cronin, S.J., Németh, K., Procter, J.N. and Zernaki, A. (2019): Volcanism in a rapidly changing environment relating to an atypical plate margin. in *Field Trip Guide for the Fifth International Volcano Geology Workshop (IAVCEI), Palmerston North (25 Feb–4 Mar)* edited by Németh, K. and Kósik, S., *Geoscience Society of New Zealand Miscellaneous Publication*, **152**, 108–203.

Leonard, G.S., Begg, J.G. and Wilson, C.J.J. (compilers) (2010): Geology of the Rotorua area: scale 1:250,000. Institute of Geological and Nuclear Sciences 1: 250,000 geological map, **5**. 1 sheet and 99p.

Lowe, D.J. (1988): Stratigraphy, age, composition, and correlation of late Quaternary tephras interbedded with organic sediments in Waikato lakes, North Island, New Zealand. *New Zealand Journal of Geology and Geophysics*, **31**, 125–165.

Lowe, D.J. (2010): Quaternary volcanism, tephras, and tephra-derived soils in New Zealand: An introductory review. *Soil and Earth Sciences Occasional Publication No. 3*, Massey University, Palmerston North, 7–29.

Lowe, D.J. (2011): Tephrochronology and its application: A review. *Quaternary Geochronology*, **6**, 107–153.

Lowe, D.J. and de Lange, W.P. (2000): Volcano-meteorological tsunamis, the *c*. AD 200 Taupo eruption (New Zealand) and the possibility of a global tsunami. *Holocene*, **10**, 401–407.

Lowe, D.J. and Green, J.D. (1992): Lakes. in *Landforms of New Zealand, 2nd edition* edited by Soons, J.M. and Selby, M.J., Longman Paul, Auckland, 107–143.

Lowe, D.J. and Newnham, R.M. (2004): Role of tephra in dating Polynesian settlement and impact, New Zealand. *Past Global Changes*, **12**(3), 5–7.

Lowe, D.J. and Palmer, D.J. (2005): Andisols of New Zealand and Australia. *Journal of Integrated Field Science*, **2**, 39–65.

Lowe, D.J. and Pittari, A. (2014): An ashy septingentenarian: The Kaharoa tephra turns 700 (with notes on its volcanological, archaeological, and historical importance). *Geoscience Society of New Zealand Newsletter*, **13**, 35–46.

Lowe, D.J. and Pittari, A. (2019): Pyroclastic flow deposits, Hinuera Valley, central North Island, and note on usage of ignimbrite as building material. *Geoscience Society of New Zealand Journal of the Historical Studies Group*, **61**, 6–15.

Lowe, D.J., Newnham, R.M., McFadgen, B.G. and Higham, T.F.G. (2000): Tephras and New Zealand archaeology. *Journal of Archaeological Science*, **27**, 859–870.

Lowe, D.J., Newnham, R.M. and McCraw, J.D. (2002): Volcanism and early Maori society in New Zealand. in *Natural Disasters and Cultural Change* edited by Torrence, R. and Grattan, J., Routledge, London, 126–161.

Lowe, D.J., Blaauw, M., Hogg, A.G. and Newnham, R.M. (2013): Ages of 24 widespread tephras erupted since 30,000 years ago in New Zealand, with re-evaluation of the timing and palaeoclimatic implications of the late-glacial cool episode recorded at Kaipo bog. *Quaternary Science Reviews*, **74**, 170–194.

Lowe, D.J., Balks, M.R. and Laubscher, N. (2014): Once despised now desired: Innovative land use and management of multilayered Pumice Soils in the Taupo and Galatea areas, central North Island, New Zealand. *Guidebook for Field Trip "Hot Vol-*

canic Soils", New Zealand Society of Soil Science Biennial National Conference, Hamilton (1–4 December), 85p.

Lube, G., Breard, E.C.P., Jons, J., Fullard, L., Dufek, J., Cronin, S.J. and Wang, T. (2019): Generation of air lubrication within pyroclastic density currents. *Nature Geoscience*, **12**, 381–386.

Manville, V. (2001): Sedimentology and history of Lake Reporoa: An ephemeral supra-ignimbrite lake, Taupo Volcanic Zone, New Zealand. *Special Publication of the International Association of Sedimentology*, **30**, 109–140.

Manville, V. (2002): Sedimentary and geomorphic responses to ignimbrite emplacement: Readjustment of the Waikato River after the A.D. 181 Taupo eruption, New Zealand. *Journal of Geology*, **110**, 519–541.

Manville, V., White, J.D.L., Houghton, B.F. and Wilson, C.J.N. (1999): Paleohydrology and sedimentology of a post-1.8 ka breakout flood from intracaldera Lake Taupo, North Island, New Zealand. *Geological Society of America Bulletin*, **111**, 1435–1447.

Manville, V., Newton, E.H. and White, J.D.L. (2005): Fluvial responses to volcanism: Resedimentation of the 1800a Taupo ignimbrite eruption in the Rangitaiki River catchment, North Island, New Zealand. *Geomorphology*, **65**, 49–70.

Manville, V., Hodgson, K.A. and Nairn, I.A. (2007): A review of break-out floods from volcanogenic lakes in New Zealand. *New Zealand Journal of Geology and Geophysics*, **50**, 131–150.

Manville, V., Swegschneider, B., Newton, E., White, J. D. L., Houghton, B.F. and Wilson, C.J.N. (2009): Environmental impact of the 1.8 ka Taupo eruption, New Zealand: Landscape responses to a large-scale explosive rhyolite eruption. *Sedimentary Geology*, **220**, 318–336.

Marshall, P. (1932): Notes on some volcanic rocks of the North Island of New Zealand. *New Zealand Journal of Science and Technology*, **11**, 198–202.

Marshall, P. (1935): Acid rocks of the Taupo-Rotorua volcanic district. *Transactions of the Royal Society of New Zealand*, **64**, 323–366.

McClelland, E., Wilson, C.J.N. and Bardot, L. (2004): Paleotemperature determinations for the 1.8-ka Taupo ignimbrite, New Zealand, and implications for the emplacement history of a high-velocity pyroclastic flow. *Bulletin of Volcanology*, **66**, 492–513.

McDaniel, P.A., Lowe, D.J., Arnalds, O. and Ping, C.-L. (2012): Andisols. in *Handbook of Soil Sciences, 2nd edition. Vol. 1: Properties and Processes* edited by Huang, P.M., Li, Y. and Sumner, M.E., CRC Press, Boca Raton, FL, 33.29–33.48.

Palmer, J.G., Ogden, J. and Patel, R.N. (1988): A 426-year floating tree-ring chronology from Phyllocladus trichomanoides buried by the Taupo eruption at Pureora, central North Island, New Zealand. *Journal of the Royal Society of New Zealand*, **18**, 407–415.

Palmer, D.J., Lowe, D.J., Payn, T.W., Höck, B.K., McLay, C.D.A. and Kimberley, M.O. (2005): Soil and foliar phosphorus as indicators of sustainability for *Pinus radiata* plantation forestry in New Zealand. *Forest Ecology and Management*, **220**, 140–154.

Pullar, W.A., Kohn, B.P. and Cox, J.E. (1977): Air-fall Kaharoa Ash and Taupo Pumice, and sea-rafted Loisels Pumice, Taupo Pumice, and Leigh Pumice in northern and eastern parts of the North Island, New Zealand. *New Zealand Journal of Geology and Geophysics*, **20**, 697–717.

Rijkse, W.C. and Vucetich, C.G. (1980): Soils of Wairakei Research Station, North Island, New Zealand. *New Zealand Soil Survey Report*, **57**, 26p.

Scott, J.M. and Molloy, A.M. (2012): The discovery of vitamin B_{12}. *Annals of Nutrition and Metabolism*, **61**, 239–245.

Segschneider, B., Landis, C.A., White, J.D.L., Wilson, C.J.N. and Manville, V. (2002): Resedimentation of the 1.8 ka Taupo ignimbrite in the Mohaka and Ngaruroro river catchments, Hawke's Bay, New Zealand. *New Zealand Journal of Geology and Geophysics*, **45**, 85–101.

Selby, M.J. (1972): The relationships between land use and erosion in the central North Island, New Zealand. *Journal of Hydrology (NZ)*, **11**, 73–87.

Selby, M.J. and Hosking, P.J. (1973): The erodibility of pumice soils of the North Island, New Zealand. *Journal of Hydrology (NZ)*, **12**, 32–56.

Selby, M.J. and Lowe, D.J. (1992): The middle Waikato Basin and hills. in *Landforms of New Zealand, 2nd edition* edited by Soons, J.M. and Selby, M.J., Longman Paul, Auckland, 233–255.

Sigl, M., McConnell, J.R., Layman, L., Maselli, O., McGwire, K., Pasteris, D., Dahl-Jensen, D., Steffensen, J.P., Vinther, B., Edwards, R., Mulvaney, R. and Kipfstuhl, S. (2013): A new bipolar ice core record of volcanism from WAIS Divide and NEEM and implications for climate forcing of the last 2000 years. *Journal of Geophysical Research: Atmospheres*, **118**, 1151–1169.

Smith, R.C.M. (1991): Post-eruption sedimentation on the margin of a caldera lake, Taupo Volcanic Centre, New Zealand. *Sedimentary Geology*, **4**, 89–138.

Smith, R.T. and Houghton, B.F. (1995a): Vent migration and changing eruptive style during the 1800a Taupo eruption: New evidence from the Hatepe and Rotongaio phreatoplinian ashes. *Bulletin of Volcanology*, **57**, 432–439.

Smith, R.T. and Houghton, B.F. (1995b): Delayed deposition of plinian pumice during Phreatoplinian volcanism: The 1800-yr-B.P. Taupo eruption, New

Zealand. *Journal of Volcanology and Geothermal Research*, **67**, 22l–226.
Soil Survey Staff (1999): *Soil Taxonomy, 2nd edition*. United States Department of Agriculture Natural Resources Conservation Service Agriculture Handbook No. 436, 869p.
Soil Survey Staff (2014): *Keys to Soil Taxonomy, 12th edition*. United States Department of Agriculture Natural Resources Conservation Service, Washington D.C., 360p.
Sparks, R.S.J., Self, S. and Walker, G.P.L. (1973): Products of ignimbrite eruptions. *Geology*, **1**, 115–118.
Stothers, R.B. and Rampino, M.R. (1983): Volcanic eruptions in the Mediterranean before A.D. 630 from written and archaeological sources. *Journal of Geophysical Research: Solid Earth*, **88**, 6357–6371.
Talbot, J.P., Self, S. and Wilson, C.J.N. (1994): Dilute gravity current and rain-flushed ash deposits in the 1.8 ka Hatepe Plinian deposit, Taupo, New Zealand. *Bulletin of Volcanology*, **56**, 538–551.
Trolese, M., Cerminara, M., Ongaro, T.E. and Giordano, G. (2019): The footprint of column collapse regimes on pyroclastic flow temperatures and plume heights. *Nature Communications*, **10**, 2476.
Vandergoes, M.J., Hogg, A.G., Lowe, D.J., Newnham, R.M., Denton, G.H., Southon, J., Barrell, D.J.A., Wilson, C.J.N., McGlone, M.S., Allan, A.S.R., Almond, P.C., Petchey, F., Dalbell, K., Dieffenbacher-Krall, A.C. and Blaauw, M. (2013): A revised age for the Kawakawa/Oruanui tephra, a key marker for the Last Glacial Maximum in New Zealand. *Quaternary Science Reviews*, **74**, 195–201.
von Lichtan, I.J., White, J.D.L., Manville, V. and Ohneiser, C. (2016): Giant rafted pumice blocks from the most recent eruption of Taupo volcano, New Zealand: Insights from palaeomagnetic and textural data. *Journal of Volcanology and Geothermal Research*, **318**, 73–88.
Walker, G.P.L. (1980): The Taupo plinian pumice: Product of the most powerful known (ultraplinian) eruption? *Journal of Volcanology and Geothermal Research*, **8**, 69–94.
Walker, G.P.L. (1981a): New Zealand case histories of pyroclastic studies. in *Tephra Studies* edited by Self, S. and Sparks, R.S.J., Reidel, Dordrecht, 317–330.
Walker, G.P.L. (1981b): The Waimihia and Hatepe plinian deposits from the rhyolitic Taupo Volcanic Centre. *New Zealand Journal of Geology and Geophysics*, **24**, 305–324.
Walker, G.P.L. (1981c): Characteristics of two phreatoplinian ashes, and their water-flushed origin. *Journal of Volcanology and Geothermal Research*, **9**, 395–407.
Walker, G.P.L. (1984): Downsag calderas, ring faults, caldera sizes, and incremental caldera growth. *Journal of Geophysical Research*, **89**, 8407–8416.
Walker, G.P.L. and Wilson, C.J.N. (1983): Lateral variations in the Taupo ignimbrite. *Journal of Volcanology and Geothermal Research*, **18**, 117–133.
Walker, G.P.L., Heming, R.F. and Wilson, C.J.N. (1980a): Low-aspect ratio ignimbrites. *Nature*, **283**, 286–287.
Walker, G.P.L., Wilson, C.J.N. and Froggatt, P.C. (1980b): Fines-deleted ignimbrite in New Zealand – the product of a turbulent pyroclastic flow. *Geology*, **8**, 245–249.
Walker, G.P.L., Self, S. and Froggatt, P.C. (1981a): The ground layer of the Taupo ignimbrite: A striking example of sedimentation from a pyroclastic flow. *Journal of Volcanology and Geothermal Research*, **10**, 1–11.
Walker, G.P.L., Wilson, C.J.N. and Froggatt, P.C. (1981b): An ignimbrite veneer deposit: The trailmarker of a pyroclastic flow. *Journal of Volcanology and Geothermal Research*, **9**, 409–421.
Watts, C.H., Marra, M.J., Green, C.J., Hunt, L.A. and Thornburrow, D. (2019): Comparing fossil and extant beetles in central North Island forests, New Zealand. *Journal of the Royal Society of New Zealand*, **49**, 474–493.
Wilmshurst, J.M. and McGlone, M.S. (1996): Forest disturbance in the central North Island, New Zealand, following the 1850 BP Taupo eruption. *Holocene*, **6**, 399–411.
Wilmshurst, J.M., Anderson, A.J., Higham, T.F.G. and Worthy, T.H. (2008): Dating the late prehistoric dispersal of Polynesians to New Zealand using the commensal Pacific rat. *Proceedings of the National Academy of Sciences of the United States*, **105**, 7676–7680.
Wilson, C.J.N. (1985): The Taupo eruption, New Zealand II. The Taupo ignimbrite. *Philosophical Transactions of the Royal Society, London*, A**314**, 229–310.
Wilson, C.J.N. (1993): Stratigraphy, chronology, styles, and dynamics of late Quaternary eruptions from Taupo volcano, New Zealand. *Philosophical Transactions of the Royal Society, London*, **A343**, 205–306.
Wilson, C.J.N. (1994): Post-conference tour day 1: Hamilton-Tokaanu. in *Conference Tour Guides* edited by Lowe, D.J., International Inter-INQUA Field Conference and Workshop on Tephrochronology, Loess, and Paleopedology, University of Waikato, Hamilton, New Zealand, 74–100.
Wilson, C.J.N. (1997): Emplacement of Taupo ignimbrite. *Nature*, **385**, 306–307.
Wilson, C.J.N. (2001): The 26.5 ka Oruanui eruption, New Zealand: An introduction and overview. *Journal of Volcanology and Geothermal Research*, **112**, 133–174.
Wilson, C.J.N. (2008): Supereruptions and supervolcanoes: Processes and products. *Elements*, **4**, 20–34.

Wilson, C.J.N. and Houghton, B.F. (2004): Taupo: The eruption. *Institute of Geological and Nuclear Sciences Information Series*, **62**.
Wilson, C.J.N. and Rowland, J.V. (2016): The volcanic, magmatic and tectonic setting of the Taupo Volcanic Zone, New Zealand, reviewed from a geothermal perspective. *Geothermics*, **59**, 168–187.
Wilson, C.J.N. and Walker, G.P.L. (1981): Violence in pyroclastic flow eruptions. in *Tephra Studies* edited by Self, S. and Sparks, R.S.J., Reidel, Dordrecht, 441–448.
Wilson, C.J.N. and Walker, G.P.L. (1982): Ignimbrite depositional facies: The anatomy of a pyroclastic flow. *Journal of the Geological Society, London*, **139**, 581–592.
Wilson, C.J.N. and Walker, G.P.L. (1985): The Taupo eruption, New Zealand. I. General aspects. *Philosophical Transactions of the Royal Society, London*, **A314**, 199–228.
Wilson, C.J.N., Ambraseys, N.N., Bradley, J. and Walker, G.P.L. (1980): A new date for the Taupo eruption, New Zealand. *Nature*, **288**, 252–253.
Wilson, C.J.N., Rogan, A.M., Smith. I.E.M., Northey, D.J., Nairn, I.A. and Houghton, B.F. (1984): Caldera volcanoes of the Taupo Volcanic Zone, New Zealand. *Journal of Geophysical Research: Solid Earth*, **89**, 8463–8484.
Wilson, C.J.N., Houghton, B.F., McWilliams, M.O., Lanphere, M.A., Weaver, S.D. and Briggs, R.M. (1995): Volcanic and structural evolution of Taupo Volcanic Zone, New Zealand: A review. *Journal of Volcanology and Geothermal Research*, **68**, 1–28.
Wilson, C.J.N., Blake, S., Charlir, B.L.A. and Sutton, A.N. (2006): The 26.5 ka Oruanui eruption, Taupo volcano, New Zealand: Development, characteristics and evacuation of a large rhyolitic magma body. *Journal of Petrology*, **47**, 35–69.
Wilson, C.J.N., Gravley, D.M., Leonard, G.S. and Rowland, J.V. (2009): Volcanism in the central Taupo Volcanic Zone, New Zealand: Tempo, styles and controls. in *Studies in Volcanology: The Legacy of George Walker* edited by Thordarson, T., Self, S., Larsen, G., Rowland, S.K. and Hoskuldsson, A., *Special Publications of IAVCEI* (*Geological Society, London*), **2**, 225–247.
Winstrup, M., Vallelonga, P., Kjær, H.A, Fudge, T.J., Lee, J.E., Riis, M.H., Edwards, R., Bertler., N.A.N., Blunier, T., Brook, E.J., Buizert, C., Ciobanu, G., Conway, H., Dahl-Jensen, D., Ellis, A., Emanuelsson, B.D., Hindmarsh, R.C.A., Keller, E.D., Kurbatov, A.V., Mayewski, P.A., Neff, P.D., Pyne, R.L., Simonsen, M..F, Svensson, A., Tuohy, A., Waddington, E.D. and Wheatley, S. (2019): A 2700-year annual timescale and accumulation history for an ice core from Roosevelt Island, West Antarctica. *Climate of the Past*, **15**, 751–779.
Zielinski, G.A., Mayewski, P.A., Meeker, L.D., Whitlow, S., Twickler, M.S., Morrison, M., Meese, D., Alley, R.B. and Gow, A J. (1994): Record of volcanism since 7000 B.C. from the GISP2 Greenland ice core and implications for the volcano-climate system. *Science*, **264**, 948–952.

ニュージーランド・タウポ火山における西暦 232 ± 10 年噴火の推移

David J. LOWE* Adrian PITTARI*

西暦 232 ± 10 年の晩夏にニュージーランド北島タウポ火山で起こった噴火は，過去 5,000 年間において地球上で起こった噴火のなかでもっとも強力なものであった。噴火は数日から数週間継続し，5 つの明確な降下火砕堆積物（ユニット Y1 ～ Y5）に続いて，非常に爆発的な噴火による低アスペクト比イグニンブライト（ユニット Y6）が堆積した。降下火砕堆積物の内，ユニット Y1, Y3 および Y4 は水蒸気プリニー式噴火によって形成され，Y2 と Y5 はプリニー式噴火であった。Y5 と Y6 は一連の噴火で形成され，非常に強い Y5 噴火による噴煙柱は高度 35–40 km に達し，それが崩壊することによって非常に高速（600–900 km/h）で高温（最高 500°C）の火砕密度流が発生し，ユニット Y6 が堆積した。このイベントによる堆積物は噴火後十数分で北島中央部の約 20,000 km^2 に及ぶ範囲を覆い尽したと考えられる。また一連の噴火によるマグマ噴出量は約 35 km^3 と見積もられている。この噴火による周辺環境への影響は甚大であり，現代においても農業などの土地利用において火山ガラスを多く含み，コバルトなどの微量元素に枯渇した土壌への対策が必要となっている。

キーワード：タウポ噴火，火砕流，密度流，プリニー式噴火，水蒸気プリニー式噴火，テフラ，火山災害

* ワイカト大学理学研究科